CHARACTERIZATION OF THE IGE-INDEPENDENT PRO-INFLAMMATORY AND PRURITOGENIC TRANSCRIPTOME OF COMPOUND 48/80-MEDIATED SKIN LESIONS IN HEALTHY DOGS

by

ILEIA JEANETTE SCHEIBE

(Under the Direction of Frane Banovic)

ABSTRACT

Recently, IgE-independent pathway of mast cell and eosinophil degranulation caused by Mas-related G-protein coupled receptors (MRGPRs) activation has been discovered. It contributes to diseases such as atopic dermatitis, chronic urticaria, and rosacea. Endogenous and exogenous compounds, including substance P, compound 48/80, and somatostatin, can induce itch and inflammation by activating MGRPRs on free nerve endings and mast cells in the skin. In dogs and humans, compound 48/80 degranulates mast cells directly through MRGPR member X2 (MRGPRX2). Compound 48/80 intradermal injection in healthy dogs induced cutaneous allergic reactions in a pilot study; however, the associated activated inflammatory and pruritic pathways in the canine MRGPRX2-induced lesions have not been investigated. The purpose of this study is to characterize the molecular pathways of acute IgE-independent induced skin lesions through MRGPRX2 activation by compound 48/80 in healthy dogs and determine how these correlate to the transcriptome of naturally occurring human and canine atopic dermatitis.

INDEX WORDS: Mas-Related G Protein-Coupled Receptor, Compound 48/80, MRGPRX2, Dog, Skin, Transcriptome

CHARACTERIZATION OF THE IGE-INDEPENDENT PRO-INFLAMMATORY AND PRURITOGENIC TRANSCRIPTOME OF COMPOUND 48/80-MEDIATED SKIN LESIONS IN HEALTHY DOGS

by

ILEIA JEANETTE SCHEIBE

BS, Delaware Valley University, 2017

A Thesis Submitted to the Graduate Faculty of The University of Georgia in Partial Fulfillment of the Requirements for the Degree

MASTER OF SCIENCE

ATHENS, GEORGIA

2020

CHARACTERIZATION OF THE IGE-INDEPENDENT PRO-INFLAMMATORY AND PRURITOGENIC TRANSCRIPTOME OF COMPOUND 48/80-MEDIATED SKIN LESIONS IN HEALTHY DOGS

by

ILEIA JEANETTE SCHEIBE

Major Professor: Frane Banovic

Committee: Robert Gogal
Kristina Meichner

Electronic Version Approved:

Ron Walcott
Vice Provost for Graduate Education and Dean of the Graduate School
The University of Georgia
December 2020

DEDICATION

I dedicate this thesis work to my wonderful husband, Billy, my amazing family, and my sweet pets. For their love, encouragement, and continuous support.

ACKNOWLEDGEMENTS

I would like to sincerely thank my mentor, Dr. Frane Banovic, for his teaching, advice, and endless support throughout this program. I want to thank him for the research opportunity, which helped me find my passion for immunology in research. I appreciate him for giving me critical constructive feedback on how I can improve as a graduate student to pursue further into the immunology field as a better higher-education student. I am also very grateful for his patience with me as I struggled throughout the program with my health issues and my lack of time management skills.

I also would like to thank my committee members, Dr. Robert Gogal and Dr. Kristina Meichner, for their feedback and guidance on the thesis.

I want to express my gratitude to all the lab members, Kathy Hoover, Tara Denley, Amanda Blubaugh, and Kelsey Robinson, for their encouragement, inspiration, support, and making the lab a fun place to work.

I thank God for this incredibly rare opportunity and His faith in me to keep pushing forward through the never-ending challenging obstacles in my life. Without God, none of this would have been possible.

I am grateful for my family, Billy, Mom, Dad, Marita, Gary, and Derek, for their unwavering support, encouragement, and kind conversations through tough times.

TABLE OF CONTENTS

Page

LIST OF TABLES

Page

LIST OF FIGURES

Page

CHAPTER 1

INTRODUCTION AND LITERATURE REVIEW

IgE- Dependent Mast Cells Activation

Mast cells are long-lived tissue-resident cells and play a role in vascular homeostasis, wound healing, innate and adaptive immunity. Most importantly, mast cells are greatly known for their role in allergic and inflammatory diseases.[1,2]

Endogenous and exogenous stimuli can induce mast cell degranulation.[1] Classical allergic and itch studies have focused on immunoglobulin E (IgE)-mediated mast cell activation by environmental allergens such as bees, venom, dust mites, eggs, nuts, and pollen. In IgE-mediated reactions, antigen leads to the IgE bound crosslinking to the high-affinity IgE receptor (FcεRI) on the mast cell surface and eosinophils to induce degranulation and release mediators which induce immediate hypersensitivity skin reactions of pruritic, raised erythematous wheals (urticaria).[1,3-5]

Upon IgE-mediated activation by an antigen, mast cells release preformed mediators from pre-stored cytoplasmic granules containing biogenic amines such as histamine and serotonin, proteases such as tryptase, chymase, and/or carboxypeptidase A3, and proteoglycans (heparin, and/or chondroitin sulfates).[2-4] Activation by IgE antigen leads to the AKT, PKC, and IKK-β phosphorylation in the mast cells. The phosphorylation of the IKK-β leads to a complex formation of soluble N-ethylmaleimide-sensitive factor activating protein receptors (SNARE) proteins such as syntaxin-4 (STX4) and synaptosomal-associated protein-23 (SNAP23).[6,7] After the immediate mast cell degranulation and release of preformed mediators, mast cells initiate the

late phase reactions (LPRs), which feature a synthesis of newly formed lipid mediators (e.g., PGD2, LTB4, LTC4, LTD4, and LTE4) and a diverse spectrum of cytokines, chemokines and growth factors.[8,9] These mediators orchestrate the recruitment, tissue infiltration, and functional activation of effector cells such as circulating leukocytes, including granulocytes such as eosinophils, basophils, and neutrophils, as well as monocytes and T cells, which substantially increases the diversity of the cellular drivers of inflammation at the site of antigen challenge.[10] Mast cells are, therefore, a crucial source of mediators contributing to the initiation of LPRs. Late phase reactions occur between 6, 24, and 48 hours after immediate degranulation. The subsequent inflammatory infiltrates in LPRs are critical for the manifestation of chronic inflammation in various systemic and cutaneous diseases.[8,10] Cutaneous LPRs are clinically characterized by erythema, edema, and sometimes pruritus.[8]

Intradermal injections of anti-IgE antibodies have been used to simulate antigen-induced IgE-mediated early and LPRs. Injections of anti-IgE antibodies in the dermis induce itch in murine atopic dermatitis (AD) models[3] and in dogs have been used as a model[11] (i.e., IgE-mediated canine AD model) for pilot evaluation of anti-inflammatory drugs for naturally occurring AD.[10] Intradermal injections of anti-IgE antibodies in dogs induce immediate hypersensitive reactions characterized by erythematous wheals and LPRs which are characterized by erythema and induration at 6 and 24 hours post-injections. In the IgE-mediated canine AD model, the LPRs are histologically characterized by an influx of active neutrophils, eosinophils, lymphocytes, and mast cells in the first 6 hours, followed by T-cells and mononuclear dendritic cells infiltration at 24 hours.[8,12] A recent study by Blubaugh et al. analyzed the molecular transcriptome of canine IgE-model skin reactions in healthy dogs using next-generation RNA sequencing.[13] Late phase IgE-mediated lesions at 6 and 24 hours had

significant upregulation of proinflammatory (e.g., LTB, IL1B, PTX3, CCL2, IL6, IL8, IL18) and T helper-(Th)2 (e.g., IL4R, IL5, IL13, IL33, and POSTN) genes, as well as Th2 chemokines (CCL17, CCL24).[13] There was also a significant upregulation of genes encoding other known pruritogenic proteins and pathways, such as cathepsin S (CTSS) and CTSC, nerve growth factor (NGF), and histamine-synthesis enzyme and receptors (HDC, HRH4).[13] Pathway analysis revealed strong significant upregulation of JAK-STAT, histamine, IL4, and IL13 signaling.[13]

IgE-Independent Activation via Mas-Related G Protein-Coupled Receptors

In 2001, a comparative transcriptome analysis of wild-type and neurogenin-1-deficient mice dorsal root ganglia (DRG) discovered a new G protein-coupled receptors (GPCRs) subfamily relating to the MAS1 oncogene; thus, the encoding genes are called Mas-related GPCRs (MRGPRs).[2,14] The study described a family of MRGPRs, which comprises 18 genes and pseudogenes in humans and 50 for mice.[14]

More recently, using next-generation sequencing, all the MRGPRs have been identified in humans, mice, and dogs; humans have MRGPR D-G and X1-X4, mice have types A-H (A1-A10, B1-B5, B8, and C11), whereas dogs have MRGPR D, F, G and X2 (Table 1).[2,6,15,16] Homology analysis using BLASTP revealed that dog MRGPRX2 had the highest amino acid sequence homology to human MRGPRX2 (62% sequence homology).[17]

Table 1. List of Mas-Related G-protein Coupled receptors (MRGPRs) in mice, humans, and dogs.

Mice	Humans	Dogs
MRGPRA (A1-A10)	MRGPRD	MRGPRD
MRGPRB (B1-B5, B8)	MRGPRE	MRGPRF
MRGPRC11	MRGPRF	MRGPRG
MRGPRD	MRGPRG	MRGPRX2
MRGPRE	MRGPRX (X1-X-4)	
MRGPRF		
MRGPRG		
MRGPRH		

Most members of MRGPRs are expressed in small-diameter sensory neurons of the dorsal root ganglia (DRG), trigeminal ganglia[18], keratinocytes, and immune cells such as mast cells, T-lymphocytes[19], eosinophils [20], basophils, and dendritic cells.[6,17,21,22]

The MRGP receptors are activated by ligands with cationic properties, which function as basic secretagogues; these are basic compounds that promote mast cell secretion.[23] The varying chemical characteristics of endogenous and exogenous substances (Table 2) ranging from peptides and proteins to cysteine proteases and opioids (e.g., eosinophil proteins, host defense peptides, tropomyosin, somatostatin, peptidergic drugs) are known to activate MRGP receptors.[23-26]

The activation of MGRPRs by basic secretagogues induces mast degranulation, and the pathway is considered IgE-independent mast cell activation.[25]. An example of endogenous secretagogues would be the major basic protein from eosinophils, substance P, beta-defensins, and tropomyosin, whereas compound 48/80, mastoparan, fluoroquinolone antibiotics (e.g., ciprofloxacin), and neuromuscular blocking drugs work as exogenous secretagogues.[17,22-25,27,28]

Table 2. List of endogenous and exogenous compounds that activates Mas-Related G Protein-Coupled Receptors.

Endogenous:		**Exogenous:**
Major Basic Protein[27]		Compound 48/80[25]
Substance P[22]		Neuromuscular Blocking Drugs[23]
Beta Defensins[27]		Fluoroquinolone Antibiotics[17]
Somatostatin[25]		Venoms (e.g., mastoparan from wasp)[26]
Pituitary adenylate cyclase-activating peptide (PACAP)[25]		Peptidergic drugs[26]
Chaperonin-10[24]		Baicalin[29]
PAMP-9–20[9,26]		Phenothiazines[23]
Host Defense Peptide[6]		Opioids[6,30]
Pathogen-associated molecular pattern (PAMP) (9-20)[26]		
SLIGKV-NH2[30]		
Cortistatin-14[18]		
Vasoactive Intestinal Peptide (VIP)[18]		
Cathelicidines[18]		
Eosinophil cationic protein (ECP)[27]		
Tropomyosin 1 – 12[24]		

The MRGPRs have large structures of seven transmembrane domains receptors connected by three extracellular loops and three intracellular loops.[2,6,18] When the antigen binds

to the extracellular domains of the MRGPRs, biological responses are elicited, such as cell development, survival, metabolism, proliferation, and transmission of neuronal signals by heterotrimeric G proteins activation and β-arrestin recruitment.[2,6] As a G protein-coupled receptors, MRGPRs employ a different activation mode than the FcεRI (e.g., requires antigen, antigen-specific IgE, and FcεRI); MRGPRs trigger exocytosis directly after agonist binding (two-component-system) in a $G_{\alpha}i$ and/or $G_{\alpha}q$-dependent manner.[7,31] Analysis in the activation of the AKT, PKC, and IKK-β pathways and the complex formation of SNAP23 and STX4 has specified that they are necessary features of IgE-dependent mast cell degranulation, which are not shared with IgE-independent mast cell degranulation.[7] The FcεRI and MRGPR routes also differ regarding granule exteriorization, whereby FcεRI triggers delayed secretion with more irregularly shaped and bigger granules due to granule-granule-fusion, while MRGPRs mediates the rapid discharge of small individual granules (Figure 1).[7]

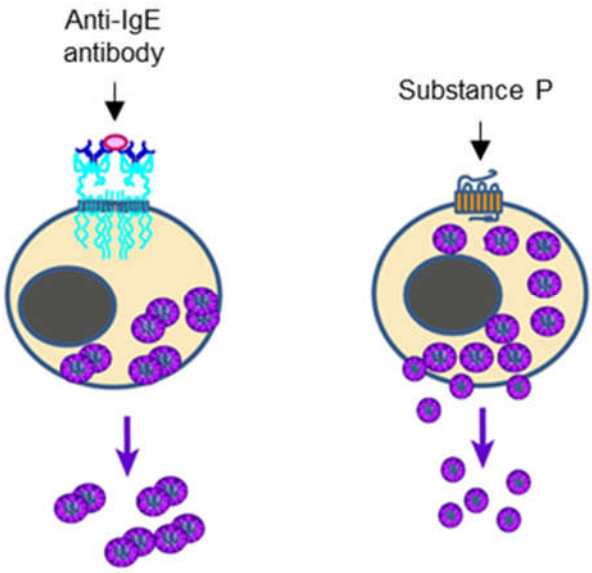

Figure 1. Modified from Bulfone-Paus *et al*., 2017.[32] Different mast cell degranulation strategies between MRGPRX2 and FcεRI by activation of substance P and anti-IgE antibody, respectively. FcεRI-mediated activation hinders the degranulation of larger and heterogenous shaped granules. Substance P activation through MRPGRX2 causes the rapid secretion of smaller and spherical-shaped granules.[7]

Importance of Mas-Related G Protein-Coupled Receptor X2 in Mast Cells and Nerves

The discovery of MRGPRX2 marks an essential change in understanding the biology of non-IgE mediated clinical phenomena on cells where MRGPRX2 is expressed (e.g., mast cells, neurons, keratinocytes, eosinophils).[20,21,33-35] Because mast cell and eosinophil activation are typically increased in allergic skin diseases such as atopic dermatitis (AD) and urticaria, the MRGPRX2 modulation by extracellular compounds (e.g., allergens) could be of great significance for the pathogenesis of the allergic diseases, and MRGPRX2 may serve as a sensor to promote inflammatory skin diseases.[23]

A comprehensive single-molecule cDNA sequencing study that included cap analysis of gene expression across 975 human samples revealed a major expression of MRGPRX2 on mast

cells, suggesting MRGPRX2 as a marker for skin-derived human MCs.[36] A recent study confirmed dominant MRGPRX2 expression on canine skin mast cells as well. Mouse MRGPRB2 is an orthologue of human MRGPRX2.[7,26,28]

In humans and dogs, MRGPRX2 is expressed by connective tissue-type mast cells, which express tryptase and chymase. Mast cells of the innate and adaptive immune system are key effector cells that regulate host defense mechanisms, and skin mast cells may account for up to 10% of all dermal immune cells.[23]

Several exogenous (e.g., compound 48/80, cationic drugs)[25,37] and endogenous ligands, like neuropeptides (e.g., substance P, cortistatin)[18,22] and host defense peptides (e.g., cathelicidins, β-defensins)[18,27] activate MRGPRX2, suggesting its broad impact in cutaneous pathophysiology.[38] Opioids, a drug class contributing to pseudo-allergy, can also target MRGPRX2; MRGPRX2 is the dominant codeine receptor in skin mast cells of humans.[23]

Although the functional activation of skin mast cells via MRGPRX2 agonists in humans has shown mast cell degranulation with a release of histamine and tryptase, the cytokine and chemokine induction by MRGPRX2 remains poorly investigated. Most MRGPRX2 functional studies were performed with LAD2 mast cells, a cell line developed over 15 years ago following marrow aspiration of a patient with aggressive mastocytosis.[39] Cytokines were detected in $CD34^+$ peripheral blood-derived cultured mast cells in one study after compound 48/80 and neuropeptide stimulation[40], while another study found that substance P stimulation showed low levels of vascular endothelial growth factor (VEGF).[7,31] It is crucial to analyze skin activation of cutaneous immune cells (e.g., mast cells, nerves, keratinocytes) via MRGRPX2 and compare cytokine and chemokine outputs in these cells to understand the functionality of MRGPRX2 in inflammatory skin diseases.

A new functional link has been recently proposed between skin nerves and MRGRPX2. Two studies identified that degranulating mast cells are mostly adjacent to activated neurons in the skin.[22,41] Furthermore, house dust mite extracts in sensitized mice induce the direct release of substance P from free nerve endings in the skin.[41] Substance P then activates murine MRGPRB2 (orthologue of human and canine MRGRPX2) on skin mast cells and dendritic cells[22], leading to activation of cells and migration to lymph nodes. This immune activation drives the type 2 skin inflammation in mice resembling spontaneous human atopic dermatitis (AD).[41]

Pathology of MRGPRs in Human Skin Diseases

Activation of mast cells via MRGPRX2 has been described to trigger degranulation, chemotaxis, and cytokine release[2], whereas the activation of MRGPRX2 on neurons induced substance P secretion from neurons[22], which then activates MRGPRX2 on the dermal immune cells. Therefore, activation of MRGPRX2 may contribute to neurogenic inflammation, pain, itch, and pruritic skin diseases. The MRGPRs have been shown to have significance in several human inflammatory skin diseases such as rosacea[6], chronic urticaria[42], atopic dermatitis, and pseudo-drug reactions by cationic drugs resulting in red man syndrome.[35]

Red Man Syndrome

Pseudo-allergic drug reactions in humans occur when a glycopeptide antibiotic like vancomycin is provided to treat gram-positive cocci infections.[35,43] Vancomycin activates MRGPRX2 inducing mast cell degranulation leading to an ailment called "red man syndrome." The "red man syndrome" is characterized by erythematous pruritic rash localized to the face, neck, and upper torso.[21,35,43-45] Swollen lips, puffy, watery eyes, dizziness, headaches, agitation, fever, and chills have also been reported to be associated with the rash.[28,44] If severe drug

reactions develop, vancomycin can cause an anaphylaxis response with nephrotoxicity, neutropenia, ototoxicity, and phlebitis.[45,40] Once these responses occur, it is recommended to discontinue vancomycin and administer diphenhydramine to terminate most of the reactions. Vancomycin should be administered slowly to minimize the risks of adverse effects.[46]

Rosacea

Rosacea is an inflammatory skin disease that features the reddening of the cheeks, forehead, chin, and can cause acne-like pustules.[6] It has been postulated that rosacea's pathogenesis is associated with microbial infections that induce significant production of cutaneous cathelicidin antimicrobial peptide LL-37. The LL-37 can activate MRGPRX2 on the mast cells and lead to sustained inflammation. Once activated, mast cells recruit neutrophils at the site of skin inflammation, which release matrix metalloproteinase-9 (MMP-9), further increasing the production of LL-37 and leading to a vicious cycle.[6] Upregulation of TRPV4 has been seen from mast cell activation and causes Gαi signaling, which allows an increase in cations influx leading to continuous mast cell degranulation through MRGPRX2.[6] Rosacea is not a life-threatening disease. However, the disease can lead to depression, thus reducing the individual's quality of life.

Chronic Urticaria

Chronic urticaria is defined as the occurrence of systemic daily wheals for at least six weeks, with mast cells playing a pivotal role in the induction of wheal reactions. The condition is known to have an autoimmune basis in 30% to 50% of patients (auto-antibodies against FcεRI)[42,47]. In contrast, the remaining approximately half of the patients have a truly "idiopathic" form of chronic urticaria. A recent study[42] revealed a significantly higher expression of MRGPRX2 in skin mast cells from patients with severe chronic urticaria compared to healthy

controls. Skin biopsies of patients with chronic urticaria show severe eosinophil infiltration and marked deposition of major basic protein, and eosinophil cationic protein, both major basic protein and eosinophil cationic protein, induce MRGPRX2 activation and rapid mast degranulation.[42] As chronic urticaria does not respond to oral antihistamine treatment in the majority of patients, the blockage of MRGPRX2 using specific inhibitors might offer a novel approach to the prevention and treatment of severe chronic urticaria.[47]

Atopic Dermatitis

Atopic dermatitis is a highly pruritic, chronic inflammatory skin disease that spontaneously develops with similar clinical phenotypes in humans and dogs.[48] In both species, AD's pathogenesis is thought to involve a complex interaction of genetic, immune, and environmental factors leading to immune dysregulation and skin barrier dysfunction.[49] Atopic dermatitis is characterized by the immune polarization of T-cell subsets (Th1/Th2/Th17/Th22), combined with differential changes in barrier proteins like filaggrin and loricrin.[50] It is unresolved to what extent IgE contributes to AD's pathogenesis; some AD patients have elevated serum IgE while others have no normal IgE values.[51] An additional factor for elevated IgE could be skin barrier impairment in AD, leading to increased bystander allergen sensitization and enhanced IgE production secondary to allergen permeation.[31] There has been a limited clinical improvement of AD with IgE-directed strategies like monoclonal antibody omalizumab and allergen-specific immunotherapy.[31] Based on the limited evidence for IgE's major contribution in AD, the MRGPR connection with AD is currently investigated in-depth. Emerging evidence suggests that mast cells and neurons form operational units[31], and AD is characterized by an increased number and activation of mast cells with subsequent clinical itch.[52] Lesional AD skin has elevated levels of substance P[23], which is an activator of MRGPRX2. In addition, the AD

skin microbiome components can stimulate antimicrobial peptide production in keratinocytes[53], of which beta-defensins and cathelicidins induce mast cell degranulation via MRGPRX2.[23] Furthermore, most AD patients are colonized with *Staphylococcus aureus* (humans) or *Staphylococcus pseudintermedius* (dogs), and its delta (δ)-toxin activates mast cells via MRGPRX2.[54,55] Finally, house dust mite allergens are the most common causative allergens worldwide[56] and can activate MRGPRX2 directly via cysteine proteases.[23]

Considering all of the potential scenarios for MRGRPX2 pathology in AD, further studies are needed to show MRGPRX2 itself or elements upstream or downstream thereof (transcription factors, signaling components) can play a significant role in spontaneous human and canine AD.

Pathology of MRGPRs in Canine Skin Diseases

Among various MRGPRs, only MRGPRX2 has been investigated for its functional biology in dogs. Canine MRGPRX2 has relatively higher sequence homology (62%) to human MRGPRX2 compared to rodents; homologies of murine MRGPRB2 and rat MRGPRB3 orthologues to human MRGPRX2 is 53% and 56%, respectively.[17]

Two recent studies[17,28] utilized transfected cells with functional MRGPRX2 to verify their ability for activation and calcium mobilization after exposure to different known ligands to active MRGPRs in humans and mice. The initial studies by Grimes *et al*. reported that compound 48/80 and several types of peptides activated dog MRGPRX2.[28] A recent study by Hamamura-Yasuno et al. expanded the initial studies on canine MRGPRs by evaluating different MRGPRs and their ligands for activation.[17] As shown before, compound 48/80 activated MRGPRX2, but not MRGPRD, F, and G[28], suggesting that canine MRGPRX2 expressed in canine connective tissues mast cells is the functional orthologue of human MRGPRX2[17].

The activation of MGRPRs in dogs and associated pathology for different canine skin diseases has been poorly investigated. In the early 1990s, a pilot study evaluated cutaneous reactions after intradermal injections of compound 48/80 in healthy dogs.[57] As previously mentioned, compound 48/80 has been shown in *in vitro* studies to activate and mediate calcium mobilization in transfected cells with human[7] and canine[17] MRGPRX2. In addition, intradermal injections of compound 48/80 induced immediate wheal and flare reactions in healthy dogs.[57] Histopathological examination of skin biopsies obtained at 20 min, 6, and 24 hours after compound 48/80 injection revealed initial mast cell degranulation followed by LPRs with eosinophils and mononuclear predominant infiltrates (monocytes, lymphocytes, macrophages).[57] Based on these findings, intradermal injections of compound 48/80 were proposed to represent canine cutaneous allergic reactions and can be used to screen novel anti-inflammatory medications for the treatment of atopic dermatitis in dogs. However, the mechanism and characterization of compound 48/80 activated inflammatory and pruritic pathways in the skin of dogs, and the correlation of these to any allergic skin condition has not been evaluated.

The purpose of this study is to characterize the molecular pathways of experimental acute IgE-independent induced skin lesions through activation of MRGPRs in healthy dogs. Identifying IgE-independent MRGPR-driven cutaneous inflammatory and itch pathways in dogs may be essential for developing novel drugs to treat allergic diseases. We hypothesize that activation of cutaneous MRGPX2 on keratinocytes, mast cells, and nerves through compound 48/80 in healthy dogs will induce a Th2 pathway response resembling naturally developing AD in humans and dogs.

CHAPTER 2

SPECIFIC AIMS

Aim 1a

The study's first aim (Aim1a) was to characterize the molecular inflammatory and pruritogenic transcriptome of acute IgE-independent compound 48/80-induced skin lesions using RNA sequencing in healthy dogs.

Aim 1b

In aim 1b, we will correlate the compound 48/80 MRGPRX2-induced lesional transcriptomes to the molecular signature of naturally occurring human and canine AD skin lesions. This comparison will allow us to understand which aspects of the spontaneous AD inflammatory profile are represented in acute MRGPRX2-induced inflammation.

CHAPTER 3

MATERIALS AND METHODS

Aim 1a. Characterization of the molecular inflammatory and pruritogenic transcriptome of acute IgE-independent compound 48/80-induced skin lesions using RNA sequencing in healthy dogs.

Animals

Eight clinically healthy male castrated research beagle dogs (age 2 to 3 years) with no previous history of pruritus, skin disease, cutaneous bacterial infections, or systemic disease were included in this study. The dogs were housed in the laboratory animal facilities at the university setting under conditions compliant with laboratory animal requirements under the University Research Animal Resources (URAR) accredited by the Association for Assessment and Accreditation of Laboratory Animal Care International (AAALAC). The sample size was determined to be sufficient to provide a 100% power to detect a significant 2-fold difference in values (mRNA transcription) between skin biopsy samples of pre- and post-compound 48/80 injections. All aspects of the study were conducted in accordance with the Institutional Animal Care and Use Committee (IACUC).

Intradermal Injections of Tested Substances, Clinical Scoring and Skin Biopsy Collections

Dogs were sedated intravenously using medetomidine (Domitor®, Pfizer, Exton, PA, USA) for all testing and biopsy procedures. It has been established that medetomidine does not interfere with intradermal skin testing reactions in dogs.[58,59] After sedation and local anesthesia

with lidocaine (Henry Schein, Dublin, OH), skin biopsies samples from healthy skin (non-injected control) at the right thoracic area were obtained seven days before the intradermal injections with compound 48/80 and saline. The thoracic area was gently clipped 48 hours before the procedure, and the skin biopsies were placed in RNAlater Stabilization Solution (Cat. No. AM7021, Ambion, Austin, TX, USA) and stored frozen at -80°C until RNA extraction. The 48-hour clipping delay prevented any skin reaction or irritation from clipping to interfere with the biopsy samples.

After seven days of initial healthy (non-injected) controls collections, the intradermal injections of compound 48/80 and phosphate-buffered saline (negative control) were performed as previously described.[57,60] As before, around 48 hours prior to injections, a large (approximately 10cm x 10cm) area for injection of the test substances was clipped on the right lateral thoracic region. Dogs were sedated intravenously using medetomidine and two 0.05 mL intradermal injections of compound 48/80 (10 micrograms/site; 0.2mg/mL; Sigma-Aldrich, St. Louis, MO, USA) and phosphate-buffered saline (PBS; Sigma-Aldrich, St. Louis, MO, USA), respectively, were administered on the right side of the thorax and evaluated by an investigator (FB). The order of injections was randomized using statistical computer software (Prism 8.0), and the investigator (FB) was blinded for the content of intradermal injections during the evaluations. The compound 48/80 concentration was chosen from the previous intradermal-induced cutaneous allergic reaction studies in dogs.[57,60]

Compound 48/80 and saline-induced cutaneous lesions were clinically scored at 20 minutes for immediate reactions (Global wheal reactions) and 6 and 24-hours post-injection (Late phase reactions). Twenty minutes after each injection, the wheals' extent and severity were assessed by the blinded investigator (FB) who performed injections. The average diameter (D)

was measured in the orthogonal direction and millimeters. Erythema (E) and firmness (F) was scored from 1 to 3 (1= no erythema/firm wheal, 2= mild erythema/moderate firm wheal, 3= strong erythema/firm wheal). Global wheal score (GWS) was calculated as GWS = D × E × F from all measurements, as previously reported. 6 and 24 hours following all intradermal injections, the late phase reactions (LPR) score was determined as LPR = E x I. Erythema, and the degree of skin induration (I) was scored from 1 to 3 (1= no erythema/induration, 2= weak erythema/induration, 3= strong erythema/induration).[61-63]

Skin biopsy samples were collected from compound 48/80-mediated and saline cutaneous reactions at 6 and 24 hours post-injection using a 6 mm standard punch biopsy (Integra-® Miltex®, York, PA, USA); saline samples served as a negative control as previously described. All biopsies were immediately bisected; one half was placed in 10% neutral buffered formalin for histopathological evaluation, and the second half was immersed immediately in RNAlater Stabilization Solution and stored at 4°C for approximately three days. RNAlater Stabilization Solution was aliquoted, and skin samples were kept frozen at -80°C until total RNA extraction.

Histopathology

Formalin-fixed paraffin-embedded skin biopsy samples were cut in one five-micrometer section and stained with hematoxylin and eosin to assess dermal inflammatory cells. All the slides were evaluated blindly, and neutrophilic, eosinophilic, and mononuclear dermal inflammation was described.

Statistical Analysis of Clinical and Histological Scoring

Results of clinical and histological scorings were statistically analyzed using GraphPad Prism 8 Software (GraphPad Software, San Diego, CA, USA). Clinical and histological scores

for GWS and LPR were compared between the control (saline) and compound 48/80 using Wilcoxon matched-pairs signed rank test with a significance level set at $P < 0.05$.

Sample Preparation for RNA Sequencing

Frozen skin biopsy samples were pulverized and placed in QIAzol Lysis Reagent (Cat. No. 79306, Qiagen, Valencia, CA, USA). Samples were homogenized using a 115V Omni TH homogenizer (Omni International, Kennesaw, GA, USA) for approximately 1 minute and furthered homogenized for another minute if needed. Total mRNA was extracted using the miRNeasy Mini Kit (Cat. No. 217004, Qiagen, Valencia, CA, USA) following the manufacturer's specifications, and each sample was eluted with 55uL of RNase-free water. RNA quantitation was evaluated using NanoDrop 2000/2000c Spectrophotometry (Thermo Fisher Scientific, Wilmington, Delaware, USA). Only RNA samples with a 260/280 ratio of ~1.8-2.0 were sent out to Novogene (Sacramento, CA, USA) for RNA quality evaluation and RNA sequencing. Only RNA samples showing a ribosomal integrity number (RIN) above seven were subjected to further analyses. All RNA samples were stored in the -80°C freezer for quantitative RT-PCR analysis.

RNA Sequencing Data Analysis

Sequencing was conducted using the Illumina platform, following the manufacturer's protocols; RNA-sequencing was performed at the Georgia Genomics Facility using an Illumina NextSeq 500, PE150 high output run. The FastQC algorithm was used for quality control assessment of the raw reads prior to trimming, and then repeated after trimming with the Trimmomatic algorithm to ensure quality was not compromised.[64,65] Trimmed reads were assessed for quality post trimming prior to alignment. Trimmed reads (in paired fq. file format)

were submitted to the Tophat2 algorithm with Bowtie2 index files for alignment-based mapping of RNA-seq reads to those splice junctions mapped out in the CanFam3.1 reference genome.[66,67]

Differential Expression Analysis and Principal Component Analysis

Cufflinks algorithms, including Cufflinks and Cuffmerge, were utilized to determine fragments per kilobase of exon model per million mapped reads (FPKM; fragments per kilobase million named shortly) values of accepted read hits from aligned RNA-seq data. The differential expression (DE) was performed on all samples using DESeq2.[68] A false discovery rate (FDR) of 0.05 or less and fold change (FC) of +/- 1.5 or greater was used for the cutoff to determine DEGs of interest for each program, and only genes meeting these criteria in all three programs were used in downstream enrichment and overlap analysis.[68,69] Differential expression analysis between different conditions (healthy non-treated, compound 48/80 and saline) was performed using empirical linear models as implemented in the R's limma package (Bioconductor, Fred Hutchinson Cancer Research Center, Seattle, Washington, USA); P values from the moderated (paired) t-test were adjusted for multiple hypotheses using the Benjamini−Hochberg procedure.[69] The $\log_2$ transformed data points were used for graphical visualization and to stabilize the variance across the means. Unsupervised hierarchical cluster analysis (HCA) and principal component analysis (PCA) were performed with data obtained from different groups using the R package. The algorithm in the default stats package in R followed calculation procedures to cluster data, incorporating Euclidean distance between each sample's data point values at the given sequence.[69] The 2D maps were generated based on these highlighted features.

Gene Set Enrichment, Gene Set Variation Analysis, Pathway Overlap Analysis and Network Analysis

Gene set enrichment analysis (GSEA) was used to weigh DEGs' significance, meeting the above criteria for differential expression with a p-value cutoff of 0.05. The AD immune (Th1, Th2, Th9, Th17, and Th22 polarizations) were quantified by using Gene Set Variation Analysis (GSVA), an unsupervised sample-wise enrichment method that produces a score of activity for a gene subset or pathways for each sample.[69 70] Modeling was performed by using the same approach described for genes, including adjustment for multiplicity.[69,71] The significantly upregulated and downregulated genes were used to ascertain pathway analysis using Metacore software (MetaCore™ version 6.32, Thomson Reuters) with median FC and FDR for all DEGs.[70] The top canonical pathways, process networks were determined based on the lowest FDR for each, respectively.[70]

Quantitative Real-Time Polymerase Chain Reaction Analysis of Selected Genes

Five upregulated and five downregulated genes from 6-hour compound 48/80 RNA sequencing were selected for quantitative real-time polymerase chain reaction (qRT-PCR). The expression levels of the selected genes were correlated with the RNA sequencing gene expression levels to verify the data. Total RNAs from skin biopsy samples were reverse-transcribed into complementary DNA (cDNA) by using the qScript cDNA SuperMix (Cat. No. 95048-500, Quantabio, Beverly, MA, USA) and the PTC-200 Gradient Thermal Cycler (MJ Research, Waltham, MA, USA). The cDNA of selected genes using forward and reverse primers (Integrated DNA Technologies, San Diego, CA, USA) was amplified with PerfaCTa SYBR Green FastMix (Cat. No. 95072-05K, Quantabio, Beverly, MA, USA) in accordance with the instructions of the manufacturer (Table 3). The list of utilized primers is available in Table 4.

The quantitative RT-PCR under the following conditions (3 minutes of initial denaturing at 95°C, then 45 cycles of 5 seconds of denaturing at 95°C, 20 seconds of annealing gradient at 45°C to 60°C, and 15 seconds of extension at 68°C to 72°C with plate read, then increments of 0.5°C from 40°C to 95°C Melt Curve with plate read for 8 seconds) was performed in a CFX96 Real-Time PCR Detection System (Bio-Rad Laboratories, Hercules, CA, USA) and in duplicates or triplicates. Cycle threshold (CT) values were standardized to the housekeeping gene ribosomal protein L8 (RPL8) and converted to fold change using the $2^{-\Delta\Delta CT}$ formula. The data were verified using Spearman's rank correlation between 6-hour compound 48/80 qRT-PCR and RNA sequencing gene fold changes.

Table 3. List of materials and volume used for 25uL reactions quantitative real-time polymerase chain reaction (qRT-PCR).

Component:	**Volume for 25uL Reaction:**
PerfeCTa SYBER Green FastMix	12.5uL
Forward Primer	0.76uL
Reverse Primer	0.76uL
Nuclease-Free Water	6.0uL
Template	5uL

Table 4. List of primers used for quantitative RT-PCR; F, forward; R, reverse; bp, base pairs; Tm, melting temperature; IL, interleukin; RPL8, ribosomal protein L8 ; LCN2, lipocalin 2; MRGPRX2, MAS-Related G Protein-Coupled Receptor family member X2; VNN1, vanin 1; CCL2, C-C motif chemokine ligand 2; TSLP, thymic stromal lymphopoietin; PTX3, pentraxin 3.

Primers:	Accession Number:	Sequence:	Tm (°C):	Product Length:
RPL8 F	XM_532360	5'- CCA TGA ATC CTG TGG AGC -3'	53.1	64bp
RPL8 R		5'- GTA GAG GGT TTG CCG ATG -3'	53.0	
IL-4 F	NM_001003159	5'- CAA CTC TGG TCT GCT TAC TA -3'	51.3	103bp
IL-4 R		5'- GCT GTG AGG ATG TTC AAC -3'	50.9	
IL-13 F	NM_001003384	5'- CCT GCT CAC CTA TGT AAG -3'	49.2	77bp
IL-13 R		5'- ACA GAT AAG GAT GCT AAG TT -3'	48.2	
IL-33 F	NM_001003180.1	5'- TAT TCA CTG CCT GTC ATC A -3'	50.8	98bp
IL-33 R		5'- TTG GAT ACT TGG AAC ATT AGC -3'	50.2	
LCN2 F	XM_022423770	5'- TAT ACC ACC ACC TAT GAG -3'	47.0	94bp
LCN2 R		5'- AAT CTC TGT TCC AGT AGT -3'	46.8	
IL-1β F	NM_001037971.1	5'- GAA GAA GAA CCT ATC ATC TG -3'	47.4	93bp
IL-1β R		5'- GCT TAT GTC CTG TAA CTT G -3'	48.0	
MRGPRX2 F	XM_005633812.2	5'- CCT GTC ATC TGT CTC CAT A -3'	50.6	127bp
MRGPRX2 R		5'- GTC ATT TAT TCA GTA AGC ATT CA-3'	49.1	
VNN1 F	NM_001003372.1	5'- CAG GAA GTG GCA TCT ATG -3'	49.9	88bp
VNN1 R		5'- AGT TGT GAG AGG AGA AGT -3'	49.7	
CCL2 F	NM_001003297	5'- ACC TGC TGC TAT ACA CTC A -3'	53.0	77bp
CCL2 R		5'- TTG CTG CTG GTG ACT CTT -3'	54.2	
TSLP F	XM_005618038.3	5'- GAG AAG GTC AAG GAA GGA -3'	50.7	83bp
TSLP R		5'- ACA CGA GAA GCA TCA GTA -3'	50.4	
PTX3 F	XM_003433174	5'- TAA GAA CAC TTG AGA CTA ATG -3'	47.2	163bp
PTX3 R		5'- AGA GAC ACA GCA CTA ATC -3'	48.5	
IL-31F	NM_001165914	5'- CTA CCA CCA AGT GAT GTA -3'	48.1	80bp
IL-31 R		5'- TTC TTC TGA TAG TCT TCC AA -3'	47.8	

Aim 1b. Perform a comparative analysis of the differentially expressed genes (DEGs) and transcriptional pathways unique to compound 48/80-induced late phase reactions at 6 hours and spontaneous human and canine AD via Spearman correlation coefficients and Metacore Overlap Analysis.

Previously Published Spontaneous Human and Canine AD Transcriptome Data

Expression data from previously published naturally developing human and canine AD transcriptomics study was reviewed and downloaded from the NCBI Gene Expression Omnibus (human AD[72] GEO: GSE121212; canine AD[73] GEO: GSE39278). The raw data were available, and data files (CEL files) were downloaded and analyzed using a battery of data quality checks[74,75] and samples failing these checks were removed from subsequent analyses. The differentially expressed genes (DEGs) were evaluated for each study set of samples individually and performed using the limma package in R. The false discovery rate (FDR) was computed as an adjusted P-value[69] to account for multiple testing, and a cutoff of 5% FDR was used to define the differential expression.

Spearman Correlation and Metacore Overlap Analysis

Correlation between significantly upregulated/downregulated DEGs (FC= +/- 1.5; FDR<0.05) of compound 48/80 skin LPRs at 6-hour and spontaneous human and canine AD lesional skin specimens were evaluated using Spearman correlation coefficients on log_2-transformed levels as previously described. Data were presented in scatterplots with estimated linear regression and a 95% confidence interval.

The DEGs data were run through Metacore software to identify the pathological pathways and process networks. Metacore overlap analysis was performed on these data to

compare compound 48/80 6-h skin lesions and spontaneous human and canine AD skin activations scores for skin samples, an FDR of 0.05 or less using the Benjamini-Hochberg procedure was used as a cutoff for a significant overlap.[23 69]

CHAPTER 4

RESULTS

Aim 1a. Characterization of the molecular inflammatory and pruritogenic transcriptome of acute IgE-independent compound 48/80-induced skin lesions using RNA sequencing in healthy dogs.

Global Wheal Score and Late Phase Reaction Scores

Intradermal injections of compound 48/80 resulted in positive wheal and erythema reactions on the right side of the thorax in all eight dogs (Figure 2b and 2c). There were no wheal and flare reactions observed after the intradermal injections of phosphate-buffered saline (control; Figure 2a). Compound 48/80 injections induced strong LPRs at 6 (Wilcoxon matched-pairs signed-rank test, p=0.0078) and 24 (p=0.0078) hours, compared to phosphate-buffered saline (Figure 3).

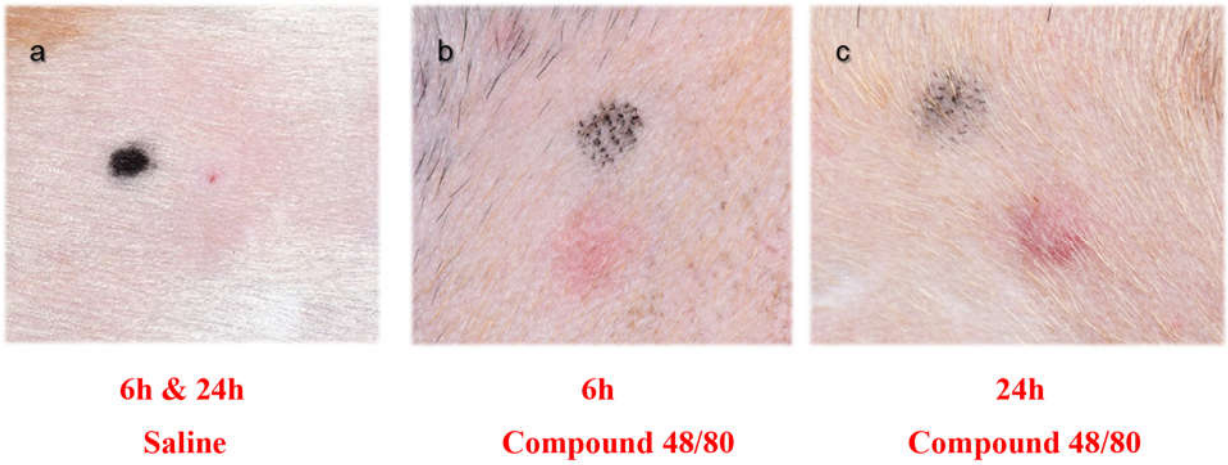

Figure 2. Clinical images of late phase reactions (LPRs) in healthy dogs after intradermal injections of phosphate-buffered saline (control, a) and compound 48/80 at 6 (b) and 24 (c) hours.

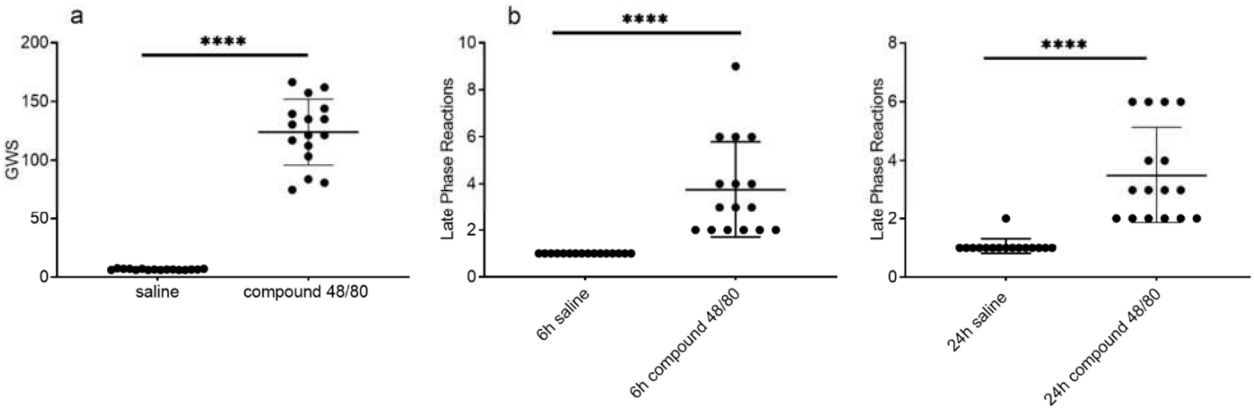

Figure 3. Global wheal scores (GWS) and late phase reaction (LPR) scores between saline and compound 48/80. Compound 48/80 induced skin lesions are significant compared to saline at $P<0.01$.

Histopathological Examination

Eosinophilic, neutrophilic, and mononuclear dermal inflammation was detected at the compound 48/80 injection sites at 6 and 24 hours; eosinophilic inflammation was strongest in 24-hours compound 48/80 skin biopsy samples from all dogs (Figure 4b and 4c). Control phosphate-buffered saline skin biopsy samples revealed mild neutrophilic and mononuclear dermal inflammation; no eosinophilic dermal inflammation was present.

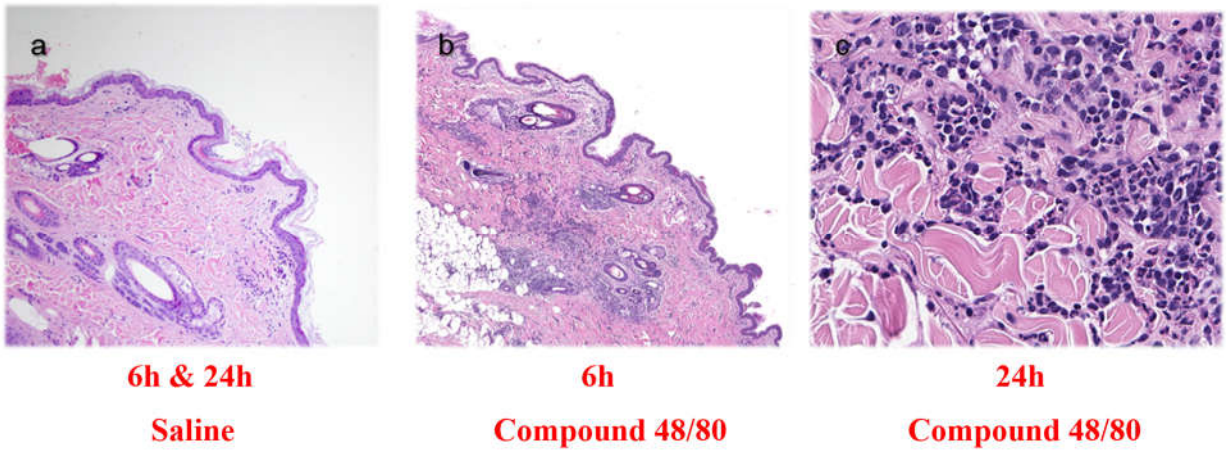

Figure 4. Histopathological examination revealed neutrophilic, eosinophilic and mononuclear inflammation in compound 48/80 injected skin (b,c) compared to saline skin (a).

RNA Sequencing: Principal Component Analysis (PCA)

Principal component analysis was utilized to analyze the distribution of all biopsy samples; PCA allows visualization of the data based on unknown phenotypes of each sample and naturally differentiates samples into groups. A clear separation of groups between healthy non-injected, saline control, and compound 48/80 at 6 hours and 24 hours was observed utilizing the 2D PCA (Figure 5 and 6); compound 48/80 induced immune activation that was significantly different than saline and healthy skin.

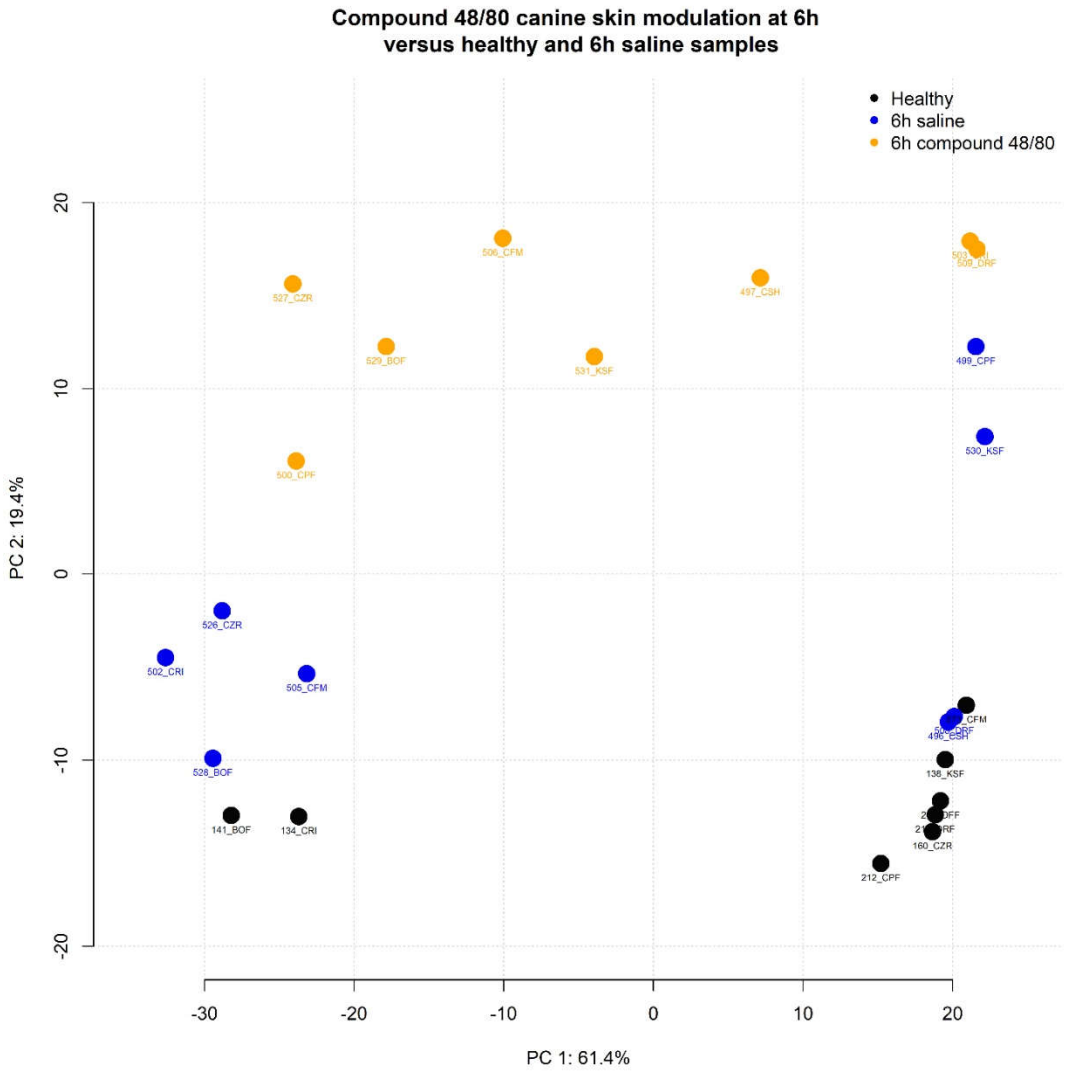

Figure 5. 2D principal component (PC) analysis plot showing the separation of each group (healthy, 6-hour saline, and 6-hour compound 48/80 samples). The PC 1 shows a 61.4% variation on the x-axis, and the second component 19.4% on the y-axis.

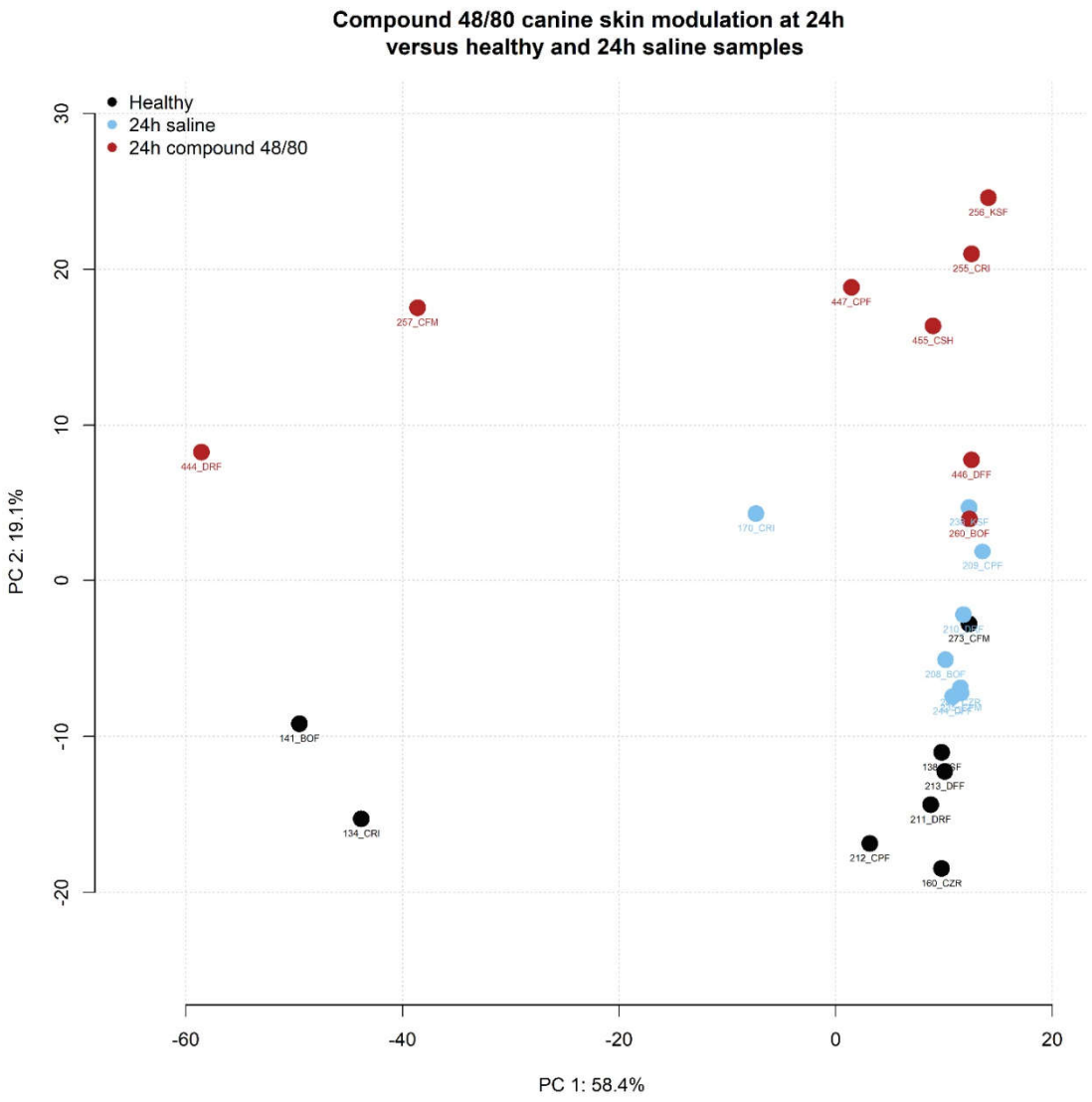

Figure 6. 2D principal component (PC) analysis plot showing the separation of each group (healthy, 24-hour saline, and 24-hour compound 48/80 samples). The PC 1 shows a 58.4% variation on the x-axis and the second component 19.1% on the y-axis.

RNA Sequencing: Differentially Expressed Genes (DEGs) Analysis

After identifying the distribution of different treatment groups with PCA, GSEA was utilized to analyze DEGs between groups. Differentially expressed genes were defined by

criteria of -1.5 ≥ FC ≥ 1.5 and FDR < 0.05 when comparing compound 48/80 6- and 24-hour vs. healthy normal skin, or saline control at 6- and 24- hours vs. respective healthy normal skin. The FC for each gene is presented based on a log base 2 form (log_2).

The comparisons of compound 48/80 vs. healthy identified a total of 4,211 and 2,899 DEGs in 6- and 24-hour compound 48/80 LPRs, respectively (Table 5). There were 1,310 and 569 DEGs in 6- and 24-hour saline control skin vs. healthy specimens, respectively (Table 5). Compound 48/80 induced three and six times more DEGs compared to saline at identical time points (Table 5).

Table 5. Differentially expressed genes (DEGs) of compound 48/80 and saline at two time points meeting the FDR<0.05 and -1.5 ≥ FC ≥ 1.5 criteria. FDR, false discovery rate; FC, fold change.

DEGs:	*6h saline*	*6h compound 48/80*	*24h saline*	*24h compound 48/80*
Total	1,310	4,211	569	2,899
Upregulated	692	2,013	300	1,853
Downregulated	618	2,198	269	1,046

We used a previously defined immune genes list to detect more specific immune phenotypic variations among compound 48/80 and saline samples.[76] Heatmap was used to depict the differences in FC-expression among compound 48/80 and saline cohorts, normalized to gene expression of respective healthy controls (Figure 7, 8, and 9).

Intradermal injections of compound 48/80 and saline induced profound proinflammatory innate immune activation of IL1B, IL6, IL8; 6h reactions were stronger than the 24h LPRs. In addition, compound 48/80 induced immune gene expression in the Th1/IFN-γ pathway; IL27, OASL, IL12A, IFNGR1, IRF1, CXCR3 were upregulated only in the compound 48/80 skin lesions.

The most significant differences between groups were in the Th2 pathway where IL5, IL13, eotaxin 2 (CCL24), RANTES (CCL5), CCR3, and STAT6 were upregulated exclusively in lesional compound 48/80 skin and not saline control. The Th2 markers IL33, IL4R, IL13RA1, and IL7R, were upregulated in the skin of both groups at 6h reactions.

The Th17 markers showed fewer differences between groups. Most Th17 markers showed mild upregulation in compound 48/80 lesional skin (IL25, IL23A, S100A12) or showed weak expression in both groups (IL17RA, LCN2, S100P, TGFB1). The dominant TH17 cytokines, IL17A and IL17F, were not upregulated in either group. However, IL17C, a keratinocyte secreting cytokine that stimulates cutaneous inflammation in atopic dermatitis and psoriasis, was significantly elevated exclusively in the compound 48/80 skin lesions.

Among the Th22 genes, only skin lesions induced by compound 48/80 showed a mild significant upregulation in several genes (IL32, S100A9/12). No significant differences were seen in the expression of IL22 among compound 48/80 and saline samples (Figure 7).

* P<0.05
**P<0.01
***P<0.001

		Fold Change			
		Saline		Compound 48/80	
		6h	24h	6h	24h
Proinflammatory					
	TNF	-1.0	1.4	1.2	1.3
	LTB	1.0	1.2	1.2	2.5 **
	IL1A	1.5	1.0	1.9 **	1.3
	IL1B	67.4 ***	3.2	62.9 ***	2.9
	IL6	109.0 ***	6.8	316.0 ***	6.6 *
	IL18	1.1	1.2	1.4 *	1.7 *
	PTX3	14.2 ***	4.6 ***	56.3 ***	3.6 ***
	IL8	37.0 ***	6.5 **	49.5 ***	5.0 **
Th1					
	CCL3	13.4 **	9.1 ***	21.0 ***	32.8 ***
	CCR1	3.6 ***	3.3 ***	22.0 ***	9.8 ***
	CCR2	1.8 *	1.3	3.0 ***	2.6 *
	CXCL10	1.4	4.7 **	2.7 *	21.7 ***
	CXCR3	1.0	1.1	-1.1	2.6 *
	IFNG	-2.1	1.4	1.9	5.6
	IL12B	-1.4	1.6	-1.4	1.7
	IL12RB2	-1.5 *	-1.1	-1.4 *	-1.3
	IRF1	1.7 *	1.5	3.4 ***	3.4 ***
	MX1	3.8 ***	20.3 ***	6.3 ***	33.6 ***
	OASL	1.4	7.3 ***	2.4 *	16.6 ***
	CCL4	3.6 *	2.2 *	5.6 ***	7.1 ***
	CCL5	-1.7	-2.1	-1.3	5.2 *
Th2					
	IL4	-1.3	-1.1	-1.3	-2.2
	IL4R	2.2 ***	1.1	3.0 ***	1.8 ***
	IL5	-1.2	1.1	2.7 *	1.0
	IL5RA	1.9	2.8	23.0 ***	58.6 ***
	IL13	1.7	-1.1	6.9 ***	1.1
	IL25	1.5	-1.1	1.1	2.5 *
	IL33	3.2 ***	1.6 *	3.1 ***	2.7 ***
	IL7R	1.6	3.5 ***	3.0 ***	5.8 ***
	STAT6	1.1	-1.0	1.0	1.3 *
	CCL17	4.5 *	2.6	1.5	2.1
	CCL7	1.9	1.5	9.0 ***	1.3

	CCR3	1.1	2.3	39.9 ***	57.7 ***
	CCR5	2.0 *	2.1 ***	3.6 ***	5.8 ***
Th17					
	IL17A	NA	-1.2	2.4	1.2
	IL17F	2.6	2.0	4.1	-1.9
	IL17RA	1.3 *	1.0	1.8 ***	1.4 ***
	IL23A	1.1	1.4	1.2	1.9 **
	IL23R	-1.1	-1.0	-1.5	-1.1
	CCL20	3.2 **	1.4	6.1 ***	-2.9 **
	IL6	109.0 ***	6.8	316.0 ***	6.6 *
	IL6R	1.3	-1.2	1.3 *	1.3
	TGFB1	1.3 **	1.1	1.6 ***	2.1 ***
	S100A8	1.6	4.2 **	1.9	3.6
	S100A9	2.8	2.8	3.9	7.0 *
	IL17C	4.4	-1.1	6.8 ***	-2.6
	S100P	-1.4	1.8 *	2.3 ***	10.3 ***
	S100A12	2.2	3.2	2.8	5.2 *
Th22					
	AHR	1.7 **	1.2	1.9 ***	1.3
	FGF5	-1.5	1.4	-1.2	-2.8 **
	IL32	-2.0	1.3	1.3	3.3 *

Figure 7. Heatmap representing fold change expression of Th polarization genes at 6-hour and 24-hour saline and compound 48/80.

Intradermal injections of compound 48/80 have been shown to induce itch in mice and dogs.[62] We evaluated the effect of intradermal injections of compound 48/80 and saline on various pruritogens in canine skin. Compound 48/80-induced skin lesions exhibited a significant up-regulation of genes encoding itch proteases cathepsin S (CTSS), mast cell chymase (CMA1), tryptase (TPS1), and mastin; only weak CTSS upregulation was seen with saline control injection. Several neurotrophin genes (NGF, GDNF, GFRA2, SEMA3A, RUNX1) leukotriene-

synthesis enzymes (ALOX5, ALOX5AP, and LTA4H) exhibited a significant upregulation in compound 48/80 6-hour and/or 24-hour (Figure 8).

* P<0.05
**P<0.01
***P<0.001

-10 0 10

		Fold Change			
		Saline		Compound 48/80	
Proteases and Receptors		**6h**	**24h**	**6h**	**24h**
Cathepsin C	CTSC	1.2	1.4 ***	1.4 **	2.7 ***
Cathepsin S	CTSS	1.3	2.6 ***	2.3 ***	7.8 ***
Chymase	CMA1	-1.1	1.1	-1.5	1.9 *
Tryptase	LOC100049001	1.1	1.3	-1.3	2.2 **
Mastin	LOC448801	1.2	1.7	1.0	3.4 ***
Histamine and Receptors					
Histidine decarboxylase	HDC	2.1 *	2.3 **	1.4	3.5 ***
Histamine N-methyltransferase	HNMT	-1.2	-1.1	-1.4 *	1.5 **
Histamine Receptor H1	HRH1	1.4	1.1	1.9 ***	1.2
Histamine Receptor H2	HRH2	2.0 ***	1.1	5.0 ***	1.2
Histamine Receptor H3	HRH3	-1.0	-1.5	-1.4	1.1
Histamine Receptor H4	HRH4	-1.4	-2.0	2.2	-1.3
Neurotrophin and Receptors					
Nerve Growth Factor	NGF	2.5	1.1	2.6 **	2.4 *
Neurotrophic Receptor Tyrosine Kinase 1	NTRK1	1.6	-1.1	1.7	1.4
Leukotrienes and Receptors					
Arachidonate 5-lipoxygenase	ALOX5	1.2	-1.0	1.3	1.9 *
Leukotriene B4 Receptor 2	LTB4R2	1.3	1.2	2.7 ***	1.6 *
Cysteinyl Leukotriene Receptor 1	CYSLTR1	-1.1	1.9 *	1.1	4.4 ***
Cysteinyl Leukotriene Receptor 2	CYSLTR2	1.4	1.2	1.4	2.1 *
Arachidonate 5-lipoxygenase-activating Protein	ALOX5AP	-1.0	1.1	1.1	2.2 ***

Figure 8. Fold change expression of pruritogen genes at 6-hour and 24-hour saline and compound 48/80 heatmap.

Epidermal barrier dysfunction is characterized by down-regulation of genes associated with lipid metabolism, the epidermal differentiation complex (EDC), and cornified envelope (CE) and tight junctions (i.e., claudins [CLDNs]). Several EDC (FLG2, TGM1, LOR) and CE (CCHCR1, EVPL, TGM3, PPL, CSTA, SCEL, CST6) genes showed significant downregulation in saline and compound 48/80 –induced skin lesions. In addition, a few epidermal lipid genes (FABP4, FADS2) exhibited a significant downregulation in saline and compound 48/80 – induced skin lesions. Finally, several tight junctions genes (CLDN1, CLDN10, CLDN5, CLDN23) showed a significant downregulation in saline and compound 48/80 -induced skin lesions (Figure 9).

* P<0.05
**P<0.01
***P<0.001

-10 **0** **10**

		Fold Change			
		Saline		Compound 48/80	
EDC (Epidermal Differentiation Complex)		**6h**	**24h**	**6h**	**24h**
	FLG	1.3	-1.3	1.1	1.1
	FLG2	1.2	-1.4 **	-1.4 *	-1.0
	TGM1	1.1	-1.2 *	-1.4 **	-1.0
	LOR	-1.2	-1.5 ***	-1.7 *	2.2 *
	IVL	-1.5	1.3	-1.1	-1.2
	TCHH	-1.4	1.2	-1.2	-2.9 *
	S100A10	-1.1	1.2 **	-1.2 **	2.1 ***
	S100A14	-1.2 *	-1.0	-1.3 *	1.3
	S100A4	-1.3	-1.0	-1.8 ***	2.4 ***
	S100A11	-1.1	1.3 ***	1.1	2.0 ***
	S100A2	-1.5 *	1.8 ***	-1.1	1.6
	S100A9	2.8	2.8	3.9	7.0 *
	KRT1	1.3	1.1	1.1	1.8 ***
	KRT10	1.4 *	1.0	1.1	2.0 ***
	KRT5	1.1	1.3 **	1.2 *	1.3
	CASP14	1.9 **	1.2	2.2 *	1.9 *
	TGM3	-1.1	-1.2	-1.6 *	2.5 **
	TGM5	1.1	-1.3	-1.0	1.1

CE (Cornified Envelope)					
	PI3	-1.3	-1.6	-1.3	1.4
	TGM1	1.1	-1.2 *	-1.4 **	-1.0
	CTSD	1.2 *	1.1	1.4 **	1.6 *
	CCHCR1	-1.1	-1.1	-1.5 ***	1.3
	EVPL	1.2	-1.1	-1.2	1.4
	TGM3	-1.1	-1.2	-1.6 *	2.5 **
	PPL	1.2 *	-1.1	-1.3 **	-1.0
	ANXA1	1.1	1.2 *	1.1	1.3 ***
	CSTA	-1.3	-1.3 *	-1.5 *	1.6
	SCEL	1.1	-1.0	-1.6 ***	1.0
	CST6	-1.4 **	-1.2	-1.4 *	1.0
	PSORS1C2	-1.3	1.1	-1.1	-1.3
	CDSN	1.0	-1.1	-1.1	-1.1
Epidermal Lipids					
	ELOVL3	-1.3	-1.5	-1.2	-1.1
	ELOVL5	-1.0	-1.0	1.3	-1.1
	FABP4	-2.4 ***	1.0	-1.5	-2.6 ***
	FABP7	-1.1	-1.4	-1.5	1.5
	FADS1	-2.1	1.2	-1.5	-1.9
	FADS2	-1.2	1.0	-1.3 *	1.6 *
Tight Junctions (Claudins)					
	CLDN1	-1.2 **	-1.1	-1.3 ***	-1.8 ***
	CLDN10	-1.9	-1.2	-3.4 *	-3.3 **
	CLDN23	-1.2	-1.1	-1.8 ***	1.2
	CLDN5	1.3	-1.3	-1.4 *	1.6
	CLDN8	-1.7 ***	-1.5 ***	-1.3 *	-2.4 ***

Figure 9. Fold change expression of epidermal barrier genes at 6-hour and 24-hour saline and compound 48/80 heatmap.

RNA sequencing: Gene Set Variation Analysis (GSVA)

To perform pathway-level comparisons for Th polarization between the compound 48/80 and saline molecular profiles, we conducted GSVA using previously published gene sets (Figure 10 and 11). [77,78] Gene Set Variation Analysis is an unbiased hierarchical clustering to determine enrichment scores for pathways based on the nonparametric Kolmogorov-Smirnov test.

Intradermal injection of saline did not show any significant increases in the Th1-, Th2-, Th17- and Th22-related pathways. Compound 48/80 showed significantly more significant upregulation in Th1- and Th2 -regulated genes at 6 hours LPRs; in addition to Th1 and Th2, the Th17 pathways were differentially expressed at 24-hour reactions. The Th22 pathway was not differentially expressed between groups.

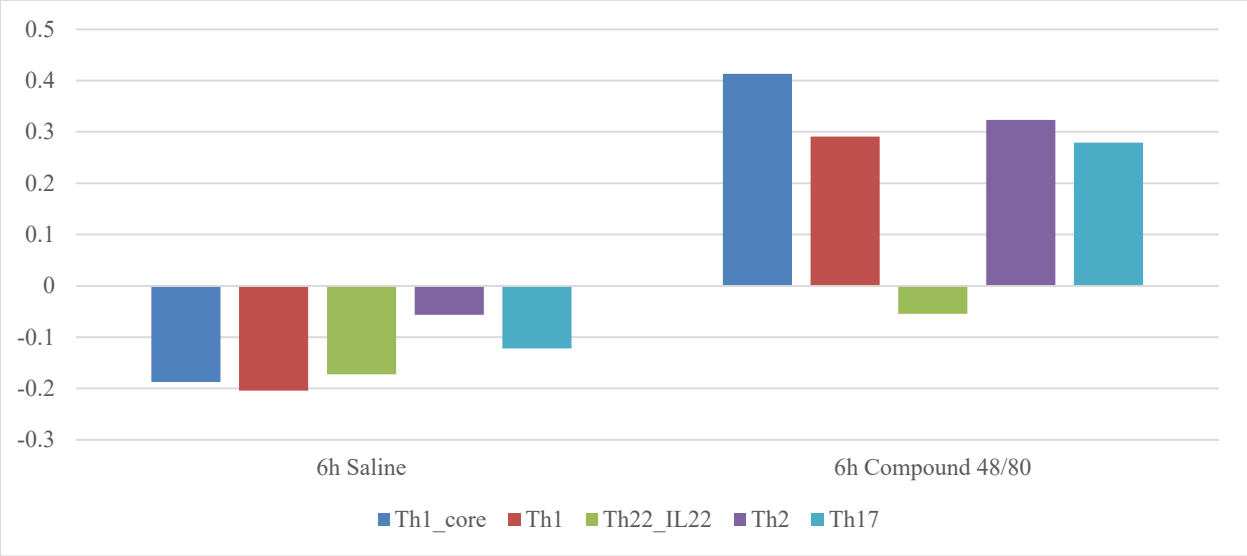

Figure 10. Gene set variation analysis (GSVA) at 6 hours, showing different T helper pathways between compound 48/80 and saline.

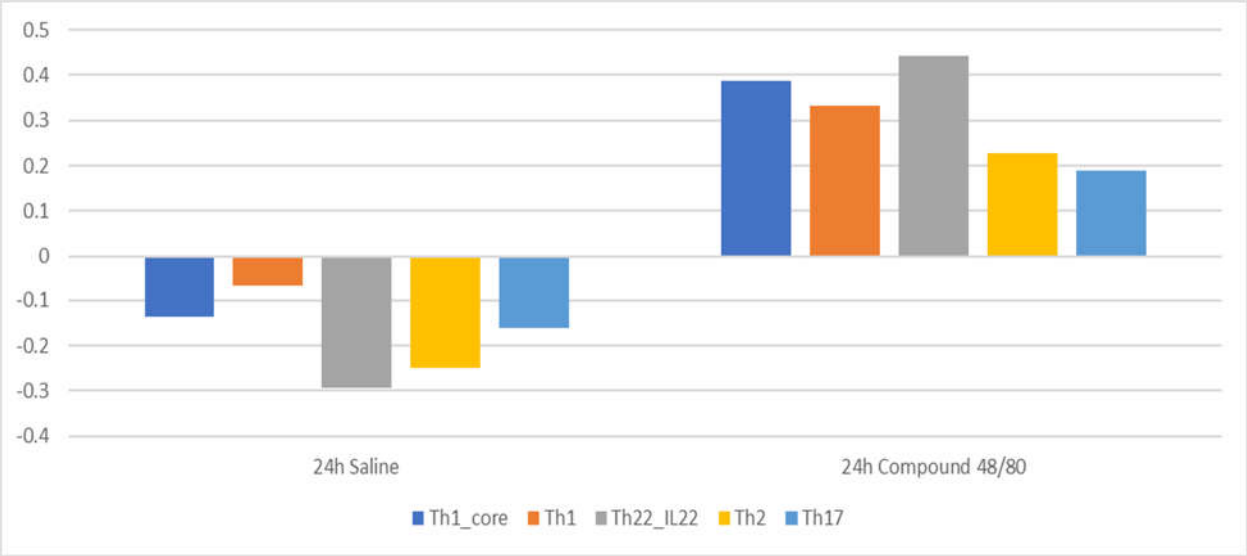

Figure 11. Gene set variation analysis (GSVA) at 24 hours, showing different T helper pathways between compound 48/80 and saline.

RNA Sequencing: Metacore Pathway Maps Within Enrichment Analysis

To understand whether the DEGs are significantly enriched in the transcriptional regulatory networks and pathway maps, DEGs were analyzed by using Metacore software. Skin lesions induced by compound 48/80 at 6 and 24-hour induced 588 and 533 significantly upregulated pathway maps, respectively (Table 6 and 7). The most upregulated pathway maps with the highest number of shared genes for compound 48/80 for both timepoints were related to migration, chemotaxis, and signaling of basophils, eosinophils, neutrophils, and mast cells. The stronger immune response of interleukin signaling pathways associated with Th2 was upregulated at compound 48/80 6h reactions, such as IL4 signaling pathway, IL4-induced

regulators of cell growth, survival, differentiation and metabolism, IL5 signaling via JAK/STAT, IL13 signaling via JAK-STAT, and IL33 signaling pathway.

Table 6. Most upregulated pathway maps of 6-hour compound 48/80 with p-values and FDR (false discovery rate).

#	Compound 48/80 6h Pathway Maps	p-value	FDR
1	Basophil migration in asthma	4.029E-20	5.959E-17
2	Cell adhesion_Integrin inside-out signaling in neutrophils	2.841E-14	1.116E-11
3	Eosinophil adhesion and transendothelial migration in asthma	5.825E-14	1.723E-11
4	Eosinophil chemotaxis in asthma	7.701E-11	6.328E-09
5	Mast cell migration in asthma	8.139E-10	4.910E-08
6	Immune response_IL-4-induced regulators of cell growth, survival, differentiation and metabolism	3.828E-08	1.205E-06
7	Immune response_IL-5 signaling via JAK/STAT	5.328E-08	1.608E-06
8	Neutrophil chemotaxis in asthma	6.329E-08	1.800E-06
9	Immune response_IL-33 signaling pathway	1.199E-07	3.112E-06
10	Immune response_IL-13 signaling via PI3K-ERK pathway	4.756E-03	1.526E-02

Table 7. Most upregulated pathway maps of 24-hour compound 48/80 with p-values and FDR (false discovery rate).

#	Compound 48/80 24h Pathway Maps	p-value	FDR
1	Basophil migration in asthma	4.654E-16	6.776E-13
2	Cell adhesion_Integrin inside-out signaling in neutrophils	3.584E-14	1.739E-11
3	Neutrophil chemotaxis in asthma	4.419E-11	1.072E-08
4	Eosinophil chemotaxis in asthma	2.497E-10	3.636E-08
5	Mast cell migration in asthma	3.093E-10	3.753E-08
6	Eosinophil adhesion and transendothelial migration in asthma	3.293E-08	2.283E-06
7	Immune response_IL-4-induced regulators of cell growth, survival, differentiation and metabolism	2.632E-06	5.987E-05
8	Immune response_IL-5 signaling via JAK/STAT	8.046E-03	2.597E-02
9	Immune response_IL-33 signaling pathway	1.088E-02	3.265E-02
10	Immune response_IL-13 signaling via PI3K-ERK pathway	4.900E-02	1.005E-01

Compound 48/80-induced reactions at 6 and 24-hours induced 35 and 49 significantly upregulated process networks, respectively (Table 8 and 9). The most upregulated process networks for compound 48/80 for both timepoints were related to the immune system, such as chemotaxis, leukocyte chemotaxis, phagocytosis, antigen presentation, innate inflammatory responses, and interferon signaling. There was also upregulation of inflammatory responses via JAK/STAT pathway, IL4 signaling, amphoterin signaling, TREM1 signaling, histamine signaling, and IgE signaling, suggesting a similar activation pathway of MRGPRX2 activation versus IgE-antigen pathway. Finally, neuronal pathways of neurogenesis axonal guidance and signal transduction via neuropeptide signaling pathways was shown in compound 48/80-induced skin lesions, confirming the functional connection between the mast activation and free nerve endings in the skin.

Table 8. Top ten process networks of 6-hour compound 48/80 with p-values and FDR (false discovery rate).

#	Compound 48/80 6h Process Networks	p-value	FDR
1	Chemotaxis	2.605E-10	4.142E-08
2	Immune response_Phagocytosis	1.977E-08	1.572E-06
3	Inflammation_Jak-STAT Pathway	6.861E-08	3.636E-06
4	Cell adhesion_Cell-matrix interactions	9.002E-07	3.578E-05
5	Cell adhesion_Leucocyte chemotaxis	1.466E-06	4.661E-05
6	Cell adhesion_Platelet-endothelium-leucocyte interactions	1.967E-06	5.212E-05
7	Inflammation_Amphoterin signaling	2.624E-06	5.216E-05
8	Proteolysis_Connective tissue degradation	2.624E-06	5.216E-05
9	Development_Blood vessel morphogenesis	1.796E-05	3.173E-04
10	Apoptosis_Anti-Apoptosis mediated by external signals via PI3K/AKT	2.548E-05	4.052E-04

Table 9. Top ten process networks of 24-hour compound 48/80 with p-values and FDR (false discovery rate).

#	Compound 48/80 24h Process Networks	p-value	FDR
1	Chemotaxis	5.069E-13	8.059E-11
2	Immune response_Phagocytosis	2.741E-11	2.179E-09
3	Cell adhesion_Leucocyte chemotaxis	5.136E-09	2.722E-07
4	Cytoskeleton_Regulation of cytoskeleton rearrangement	1.774E-07	7.052E-06
5	Inflammation_Interferon signaling	3.708E-07	9.878E-06
6	Cell adhesion_Platelet-endothelium-leucocyte interactions	3.728E-07	9.878E-06
7	Immune response_Phagosome in antigen presentation	4.396E-07	9.984E-06
8	Apoptosis_Anti-apoptosis mediated by external signals via NF-kB	1.047E-05	2.081E-04
9	Cell adhesion_Glycoconjugates	1.290E-05	2.278E-04
10	Cell adhesion_Cell-matrix interactions	1.505E-05	2.394E-04

Quantitative RT-PCR (qRT-PCR)

To validate RNA-seq findings, we performed qRT-PCR on 10 selected DEGs from compound 48/80 and saline skin lesions at 6 hours. We correlated the results between RNA-seq and qRT-PCR using the Spearman correlation coefficient. A significant moderate to very strong correlation was observed between techniques for DEGs in saline (r=0.70) and compound 48/80 (r= 0.91) skin lesions (Figure 12 and 13).

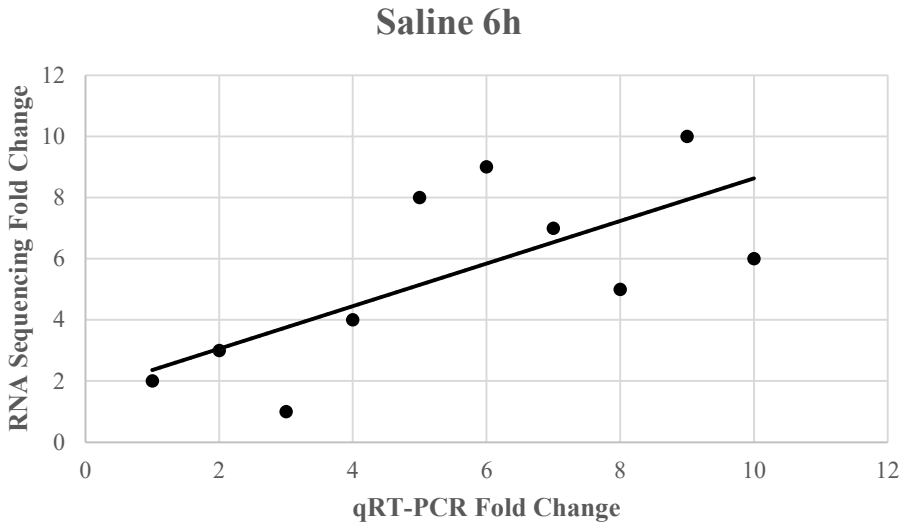

Figure 12. Spearman's rank test of saline 6-hour control gene fold changes (FC) between quantitative RT-PCR (qRT-PCR) and RNA sequencing (rho=0.70, p=0.0252).

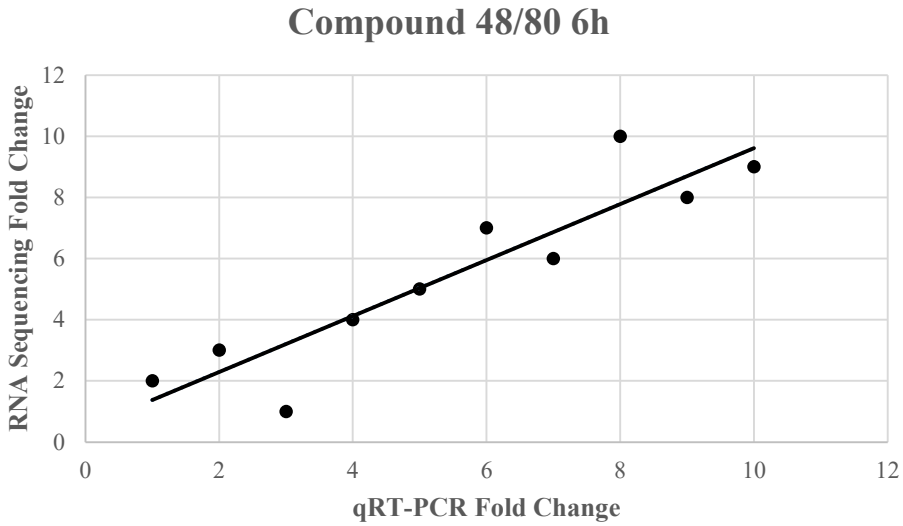

Figure 13. Spearman's rank test of compound 48/80 6-hour gene fold changes (FC) between quantitative RT-PCR (qRT-PCR) and RNA sequencing (rho= 0.91, p= 0.0002).

Aim 1b. Perform a comparative analysis of the differentially expressed genes (DEGs) and transcriptional pathways unique to compound 48/80-induced late phase reactions at 6/24 hours and spontaneous human and canine atopic dermatitis via Spearman correlation coefficients and Metacore Overlap Analysis.

Correlation Analysis of Compound 48/80 Late Phase Reactions and Spontaneous Human Atopic Dermatitis

To assess the similarity of compound 48/80-induced skin lesions and human AD skin directly, we queried human gene symbols corresponding to canine gene symbols using the bioinformatics package biomaRt. We investigated the overlap between these human orthologues of canine DEGs in compound 48/80 LPRs and a previously published transcriptome skin data from spontaneous human AD[72] using criteria of $-1.5 \geq FC \geq 1.5$ and $FDR<0.05$.

We found that the compound 48/80 LPRS at 6 and 24 hours contained 17% and 14% of human DEGs in spontaneous human AD (Figure 14 and 15), respectively. The overlap in DEGs is similar to many murine AD models for which published DEGs were available[79]; murine models are commonly used in preclinical studies from human AD. Spearman correlation coefficient for the shared DEGs between canine and humans samples revealed a significant moderate to strong positive correlation for compound 48/80 6-hour samples ($r=0.53$) and 24-hour samples ($r= 0.47$) (Figure 16 and 17).

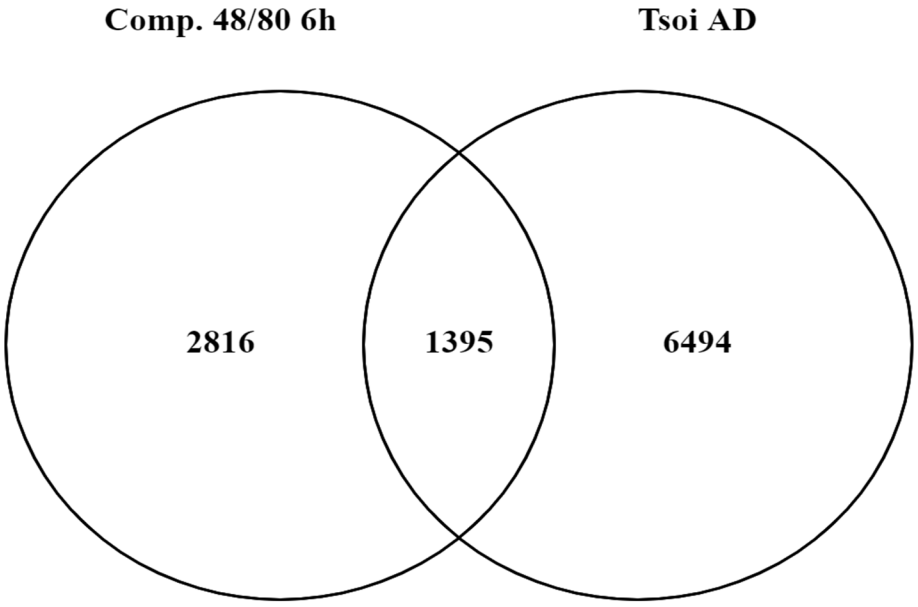

Figure 14. Venn diagram of shared differentially expressed genes (DEGs; -1.5 ≥ FC ≥ 1.5, FDR<0.05) between 6-hour compound 48/80 and spontaneous human atopic dermatitis[72]

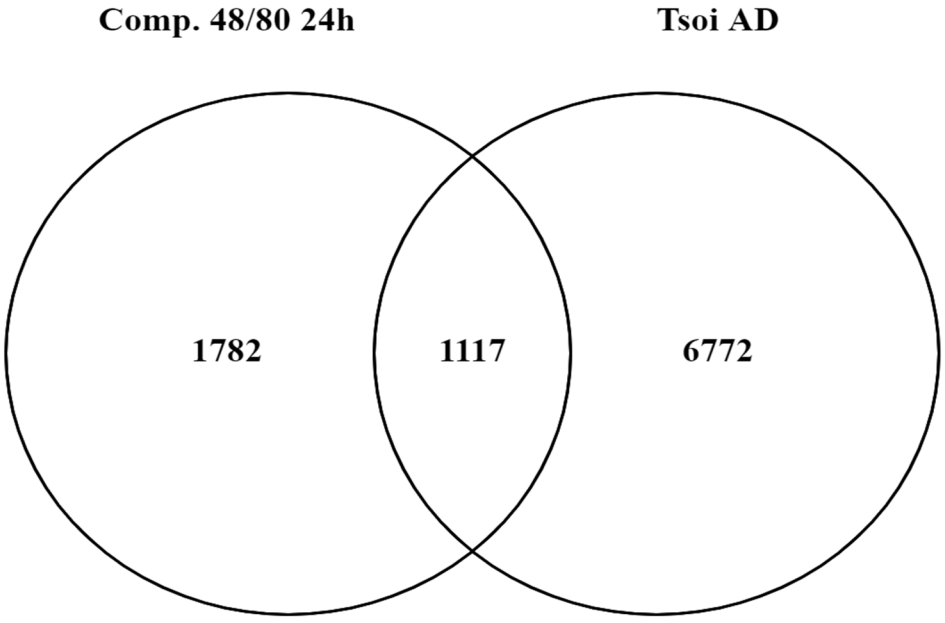

Figure 15. Venn diagram of shared differentially expressed genes (DEGs; -1.5 ≥ FC ≥ 1.5, FDR<0.05) between 24-hour compound 48/80 and spontaneous human atopic dermatitis.[72]

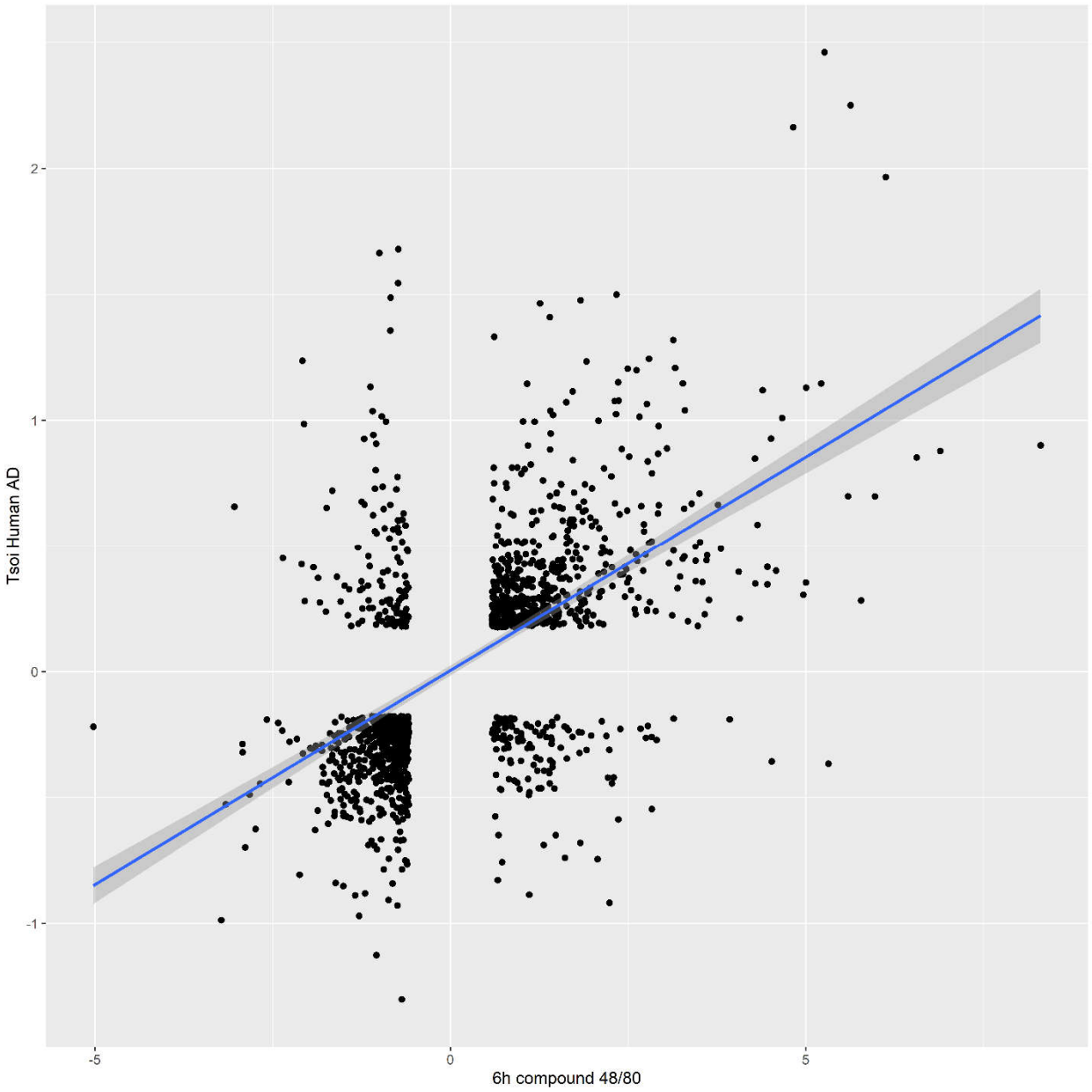

Figure 16. Spearman's rank test of differentially expressed genes (DEGs; $-1.5 \geq FC \geq 1.5$, FDR<0.05) between 6-hour compound 48/80 late phase reaction and spontaneous human atopic dermatitis[72] (AD) (rho=0.54, $p=2.2e^{-16}$).

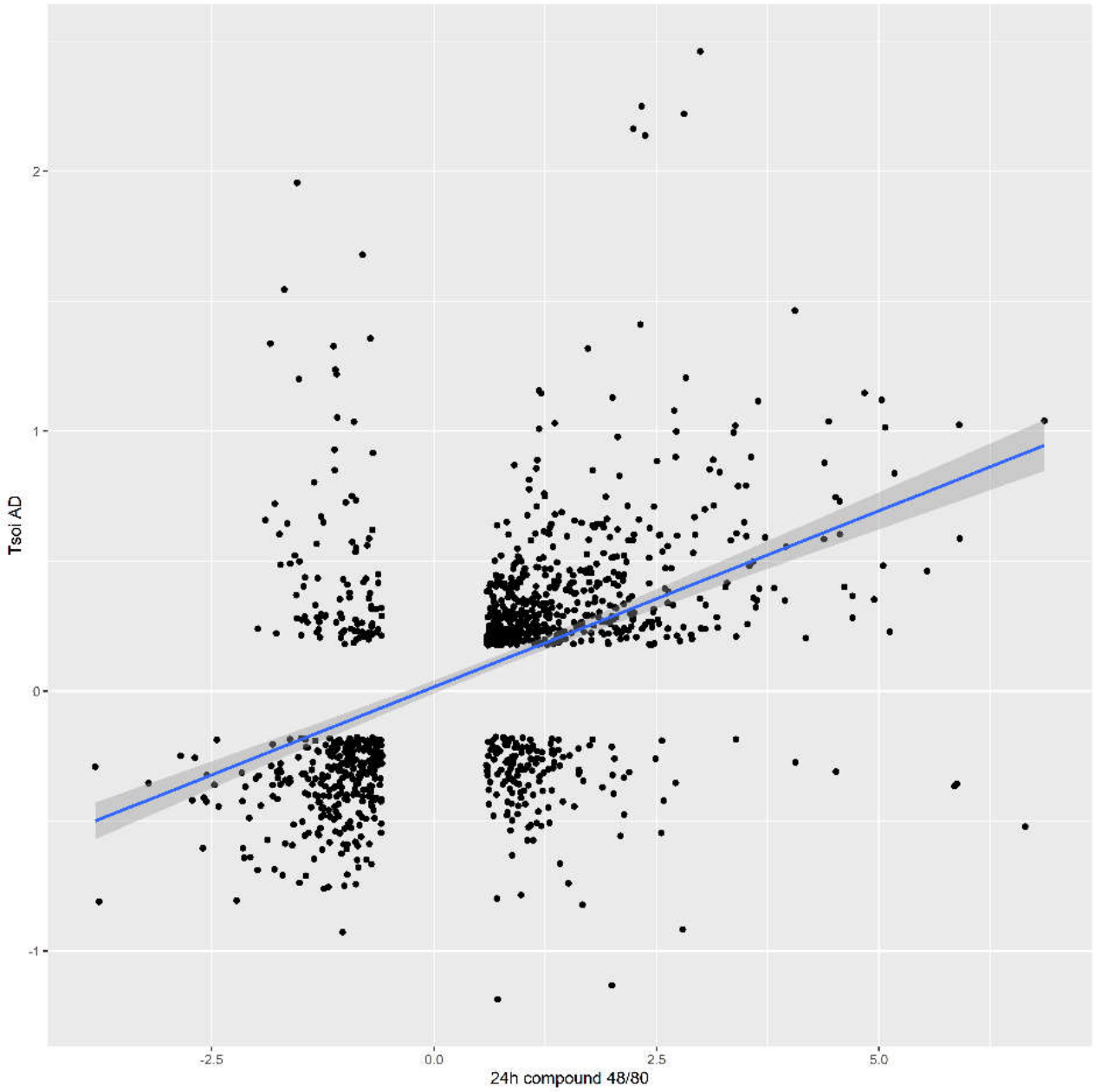

Figure 17. Spearman's rank test of differentially expressed genes (DEGs; $-1.5 \geq FC \geq 1.5$, FDR<0.05) between 24-hour compound 48/80 late phase reaction and spontaneous human atopic dermatitis[72] (AD) (rho=0.47, $p=2.2e^{-16}$).

Greatest enrichment (Metacore Overlap analysis for process networks) was observed in DEGs related to chemotaxis, leukocyte chemotaxis, phagocytosis, innate immunity, and interferon signaling (Table 10 and 11). Among overlapping genes were those important for immune pathways (JAK/STAT pathway, IL4 signaling, amphoterin signaling, TREM1 signaling, and histamine signaling) and neurophysiological and neurogenesis processes (transmission of nerve impulse, synaptogenesis, axonal guidance).

Table 10. Top ten overlap process networks between 6-hour compound 48/80 and spontaneous human AD[72] with p-values and FDR (false discovery rate).

#	Compound 48/80 6h and Tsoi AD Process Networks Overlap	p-value	FDR
1	Chemotaxis	3.174E-14	5.047E-12
2	Inflammation_Amphoterin signaling	1.984E-12	1.577E-10
3	Inflammation_Neutrophil activation	1.036E-09	5.490E-08
4	Immune response_Phagocytosis	1.486E-09	5.905E-08
5	Inflammation_Jak-STAT Pathway	2.872E-09	8.944E-08
6	Cell adhesion_Leucocyte chemotaxis	3.375E-09	8.944E-08
7	Inflammation_Histamine signaling	8.733E-09	1.984E-07
8	Development_Regulation of angiogenesis	2.368E-08	4.706E-07
9	Proteolysis_ECM remodeling	1.080E-07	1.908E-06
10	Proteolysis_Connective tissue degradation	1.336E-07	2.124E-06

Table 11. Top ten overlap process networks between 24-hour compound 48/80 and spontaneous human AD[72] with p-values and FDR (false discovery rate).

#	Compound 48/80 24h and Tsoi AD Process Networks Overlap	p-value	FDR
1	Chemotaxis	9.698E-17	1.532E-14
2	Inflammation_Amphoterin signaling	3.360E-11	2.218E-09
3	Inflammation_Neutrophil activation	4.212E-11	2.218E-09
4	Immune response_Phagocytosis	1.957E-09	7.261E-08
5	Inflammation_Jak-STAT Pathway	2.298E-09	7.261E-08
6	Cell adhesion_Leucocyte chemotaxis	8.177E-09	2.153E-07
7	Inflammation_Histamine signaling	6.895E-08	1.547E-06
8	Development_Regulation of angiogenesis	7.835E-08	1.547E-06
9	Proteolysis_ECM remodeling	2.032E-07	3.568E-06
10	Proteolysis_Connective tissue degradation	2.259E-07	3.569E-06

Correlation Analysis of Compound 48/80 Late Phase Reactions and Spontaneous Canine Atopic Dermatitis

We investigated the overlap between canine DEGs in compound 48/80 LPRs and a previously published transcriptome skin data from spontaneous canine AD[73] using criteria of $-1.5 \geq FC \geq 1.5$ and $FDR<0.05$. The transcriptome study spontaneous evaluating canine AD utilized microarray technology, which is limited by a predetermined set of genes, and some essential AD genes, unfortunately, are not represented. Transcriptome study for spontaneous human AD was performed using RNA seq, which analyzes all the genes. Thus, that explains why the transcriptome dataset from the spontaneous human AD has a larger number of DEGs than the canine AD dataset.

We found that the compound 48/80 LPRS at 6 and 24-hour contained 48% and 50% of DEGs in spontaneous canine AD (Figure 18 and 19), respectively.

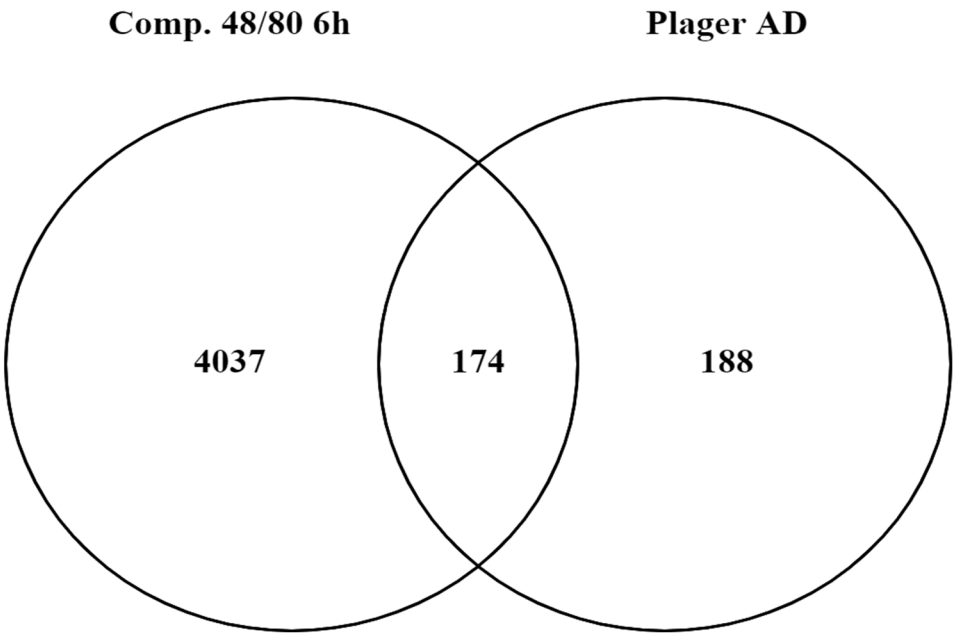

Figure 18. Venn diagram showing shared differentially expressed genes (DEGs) between 6-hour compound 48/80 late phase reactions and spontaneous canine atopic dermatitis.[73]

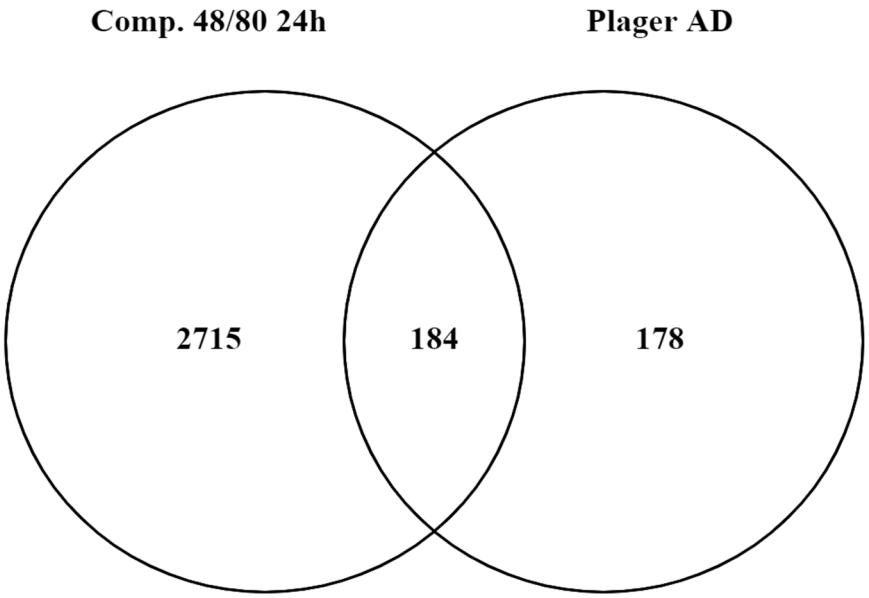

Figure 19. Venn diagram showing shared differentially expressed genes (DEGs) between 24-hour compound 48/80 late phase reactions and spontaneous canine atopic dermatitis.[73]

Spearman correlation coefficient for the shared DEGs between samples revealed a significant strong positive correlation between spontaneous canine AD and compound 48/80 6-hour samples (r=0.6) and 24-hour samples (r= 0.63) (Figure 20 and 21).

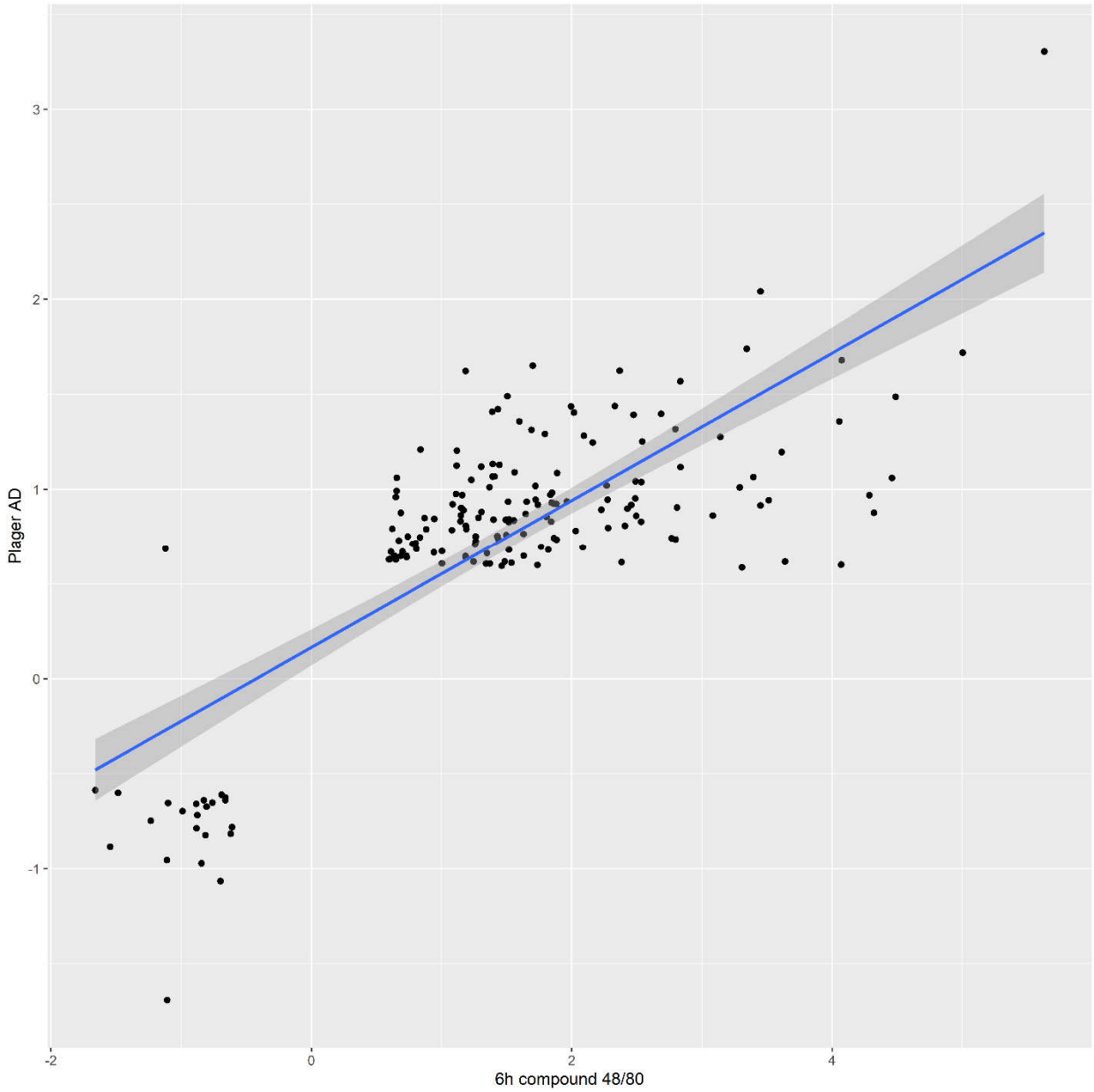

Figure 20. Spearman's rank test of differentially expressed genes (DEGs; $-1.5 \geq FC \geq 1.5$, FDR<0.05) between 6-hour compound 48/80 late phase reaction and spontaneous canine atopic dermatitis[73] (rho=0.60, $p=2.2e^{-16}$).

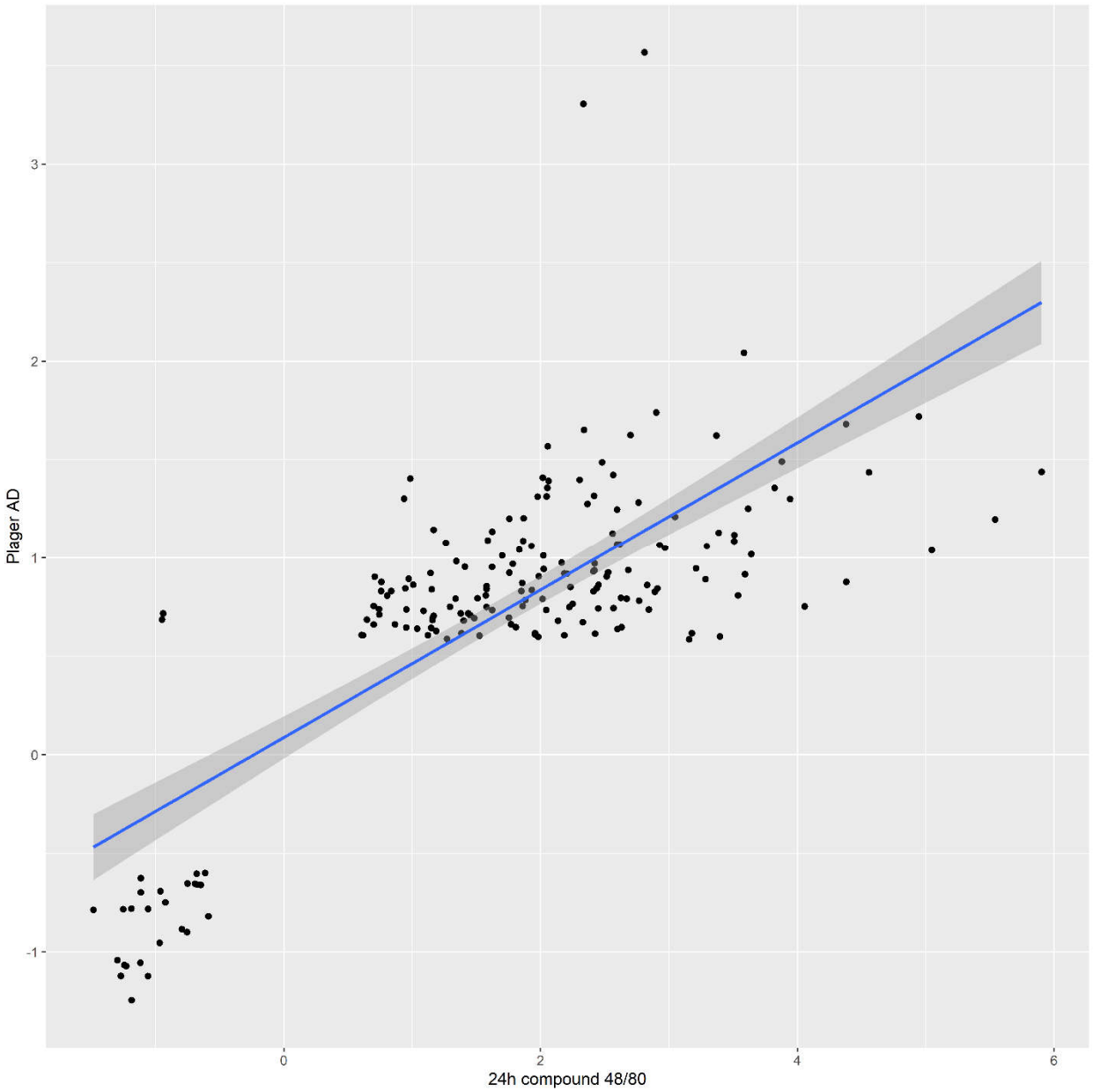

Figure 21. Spearman's rank test of differentially expressed genes (DEGs; $-1.5 \geq FC \geq 1.5$, FDR<0.05) between 24-hour compound 48/80 late phase reaction and spontaneous canine atopic dermatitis[73] (rho=0.63, $p=2.2e^{-16}$).

Metacore Overlap analysis for process networks between compounds 48/80 and spontaneous canine AD showed enrichment in 12 and 13 networks for 6- and 24- hours skin samples, respectively. Upregulated molecular pathways included pathways related to chemotaxis, innate immune inflammatory response, IL-4, JAK/STAT, TREM1, and amphoterin signaling (Table 12 and 13).

Table 12. Overlap process networks between 6-hour compound 48/80 and spontaneous canine AD[73] with p-values and FDR (false discovery rate).

#	Compound 48/80 6h and Plager AD Process Networks Overlap	p-value	FDR
1	Chemotaxis	7.253E-11	5.295E-09
2	Inflammation_Interferon signaling	2.049E-09	7.477E-08
3	Cell adhesion_Leucocyte chemotaxis	2.267E-05	5.517E-04
4	Development_Regulation of angiogenesis	9.798E-05	1.788E-03
5	Cell adhesion_Platelet-endothelium-leucocyte interactions	1.022E-03	1.354E-02
6	Inflammation_Amphoterin signaling	1.113E-03	1.354E-02
7	Immune response_Innate immune response to RNA viral infection	2.362E-03	2.464E-02
8	Inflammation_TREM1 signaling	2.766E-03	2.524E-02
9	Immune response_Th17-derived cytokines	4.129E-03	3.251E-02
10	Cell adhesion_Glycoconjugates	4.454E-03	3.251E-02

Table 13. Top ten overlap process networks between 24-hour compound 48/80 and spontaneous canine AD[73] with p-values and FDR (false discovery rate).

#	Compound 48/80 24h and Plager AD Process Networks Overlap	p-value	FDR
1	Chemotaxis	2.020E-10	9.519E-09
2	Inflammation_Interferon signaling	2.573E-10	9.519E-09
3	Cell adhesion_Leucocyte chemotaxis	4.160E-05	1.026E-03
4	Inflammation_Amphoterin signaling	1.997E-04	3.694E-03
5	Immune response_Innate immune response to RNA viral infection	3.228E-04	4.778E-03
6	Immune response_Th17-derived cytokines	6.953E-04	8.576E-03
7	Development_Regulation of angiogenesis	1.030E-03	1.088E-02
8	Inflammation_IL-4 signaling	1.431E-03	1.290E-02
9	Cell adhesion_Platelet-endothelium-leucocyte interactions	1.568E-03	1.290E-02
10	Inflammation_Jak-STAT Pathway	2.143E-03	1.586E-02

CHAPTER 5

DISCUSSION

This is the first global molecular profiling study of inflammatory skin lesions activated through MRGPRX2 in the skin of healthy dogs. Despite similar activation of proinflammatory genes in both groups, our data revealed significant variations in cellular infiltration and expression of immune and barrier genes between compound 48/80 and saline control skin lesions. All gene expression results in this study were normalized to expression in matching healthy control untreated samples. Thus, the differences in compound 48/80 and saline control detected in this study cannot be attributed to variations among healthy control groups.

Recent molecular phenotyping studies in chronic AD skin lesions of pediatric, European/American AD, and Asian AD populations have shown significant variability in Th-axis (Th1, Th2, Th17, Th22) involvement and epidermal barrier characteristics.[80] However, a strong Th2-axis up-regulation has been consistently observed across all AD populations.[50] The observed variability in these studies is likely the consequence of the different chronic disease stages of AD among populations. Historically, AD has been characterized as a biphasic disease with a Th2-to-Th1 transition from acute to chronic AD stage[81]; however, there are conflicting data. To elucidate the transition from acute to chronic AD disease stages and the factors and mechanisms that shape chronic inflammatory activity, Tsoi et al. recently performed RNA sequencing on acute and chronic AD lesions within the same individuals.[72] The results by Tsoi et al. showed that the changes accompanying the transition from nonlesional to acute to chronic

inflammation in AD are quantitative rather than qualitative; approximately 74% of the genes dysregulated in acute lesions remain or are further dysregulated in chronic lesions.[82] All the major Th1, Th2, and Th17 responses were progressively heightened from nonlesional AD to acute and then chronic AD lesions, whereas nonlesional AD was enriched in Th2 and Th17 responses.[82] The Th22 response, mediated by the dominant cytokine IL-22 responsible for epidermal hyperplasia in chronic AD skin lesions, was upregulated in both acute and chronic AD lesions.[82]

In this study, intradermal injections of compound 48/80 through activation of MRGPRX2 in healthy dogs induced acute multipolar Th polarization in the skin with early upregulation of Th1 and Th2 pathway at 6 hours and Th1, Th2, and Th17 at 24 hours. Compound 48/80 transcriptomic profile was compared with the spontaneous human[72] and canine[73] AD transcriptome to compare how well the compound 48/80-induced skin lesions vis MRGPRX2 represent human and canine AD. Previous studies utilizing murine AD-like models revealed that murine transcriptomes represent only 37%, 18%, 17%, and 11% of the human meta-analysis–derived atopic dermatitis profile for IL-23–injected, NC/Nga, oxazolone (OXA)-challenged, and ovalbumin (OVA)-challenged mice, respectively.[79] Surprisingly, there was around 30% overlap in DEGs with a good positive correlation between the transcriptome of compound 48/80 skin lesions and human AD, which is more than in several murine AD-like models. Although compound 48/80-induced lesions did not capture all immune and barrier aspects of chronic spontaneous human AD, the results of this study demonstrate that MRGPRX2 activation in skin induces a wide array of inflammatory axes, including Th2 activation, and could be suited in preclinical studies to evaluate this AD-centric axis and how it communicates with other activated cytokines in AD patients.

Histologically, acute AD skin lesions in humans and dogs exhibit spongiosis with mild to moderate acanthosis in addition to a superficial perivascular infiltrate of lymphocytes and macrophages; mast cells can show degranulation, and occasionally eosinophils may be present.[82] Compound 48/80-induced acute skin lesions featured similar changes with mild acanthosis and superficial dermis expanded by mild edema, intermixed with neutrophils, eosinophils, lymphocytes, and plasma cells; eosinophils and mononuclear cells dominated the late phase reactions at 24 hours. Eosinophil recruitment to allergic inflammation sites in the skin and other tissues is driven by IL-5 and by chemotactic chemokines, such as eotaxin-1 (CCL11) and eotaxin-2 (CCL24), monocyte chemotactic protein 3 (MCP3; CCL7), and regulated on activation, normal T cell expressed and secreted (RANTES; CCL5). These chemokines bind to eosinophils via the ß-chemokine receptor CCR3, which encourages the recruitment of eosinophils to allergic inflammation sites.[83] The significant eosinophilic inflammation in the compound 48/80 skin lesions compared to controls can be explained by the upregulation of IL5 and IL5RA as well as chemokines eotaxin-2, MCP3, and RANTES. In addition, ß-chemokine receptor CCR3 responsible for eosinophilic recruitment was strongly upregulated in both compound 48/80 time points (6 and 24 hours).

As previously mentioned, AD has a long time been considered a Th2 disease.[72] A recent study revealed that IL13 is the dominant Th2 cytokine in spontaneous acute and chronic human AD skin lesions.[72] This was a surprising finding as AD has, for a long time, been considered a Th2 disease with predominant IL4 cytokine responses.[72] The half-life of the interleukin 4 in vivo is short and shares much of its biology with the IL13 cytokine, while the heterodimeric receptor IL4R/IL13Rα of IL13 is shared with IL4.[72] Interleukin 13, along with receptors IL4R and

IL13Rα1, was the dominant Th2 cytokine in the compound 48/80 skin lesions in this study, whereas IL-4 was not affected by the MRGPRX2 activation.

Interleukin 31 is a Th2 dominant pruritogen cytokine of humans, primates, mice, and dogs. Increased IL31 serum levels have been observed in some AD dogs; there is a subset of dogs with AD that had no detectable levels of IL31 in the circulation.[69] In this study, the RNA sequencing did not show any upregulation of IL31 in compound 48/80 or saline control skin lesions. Interestingly, previous canine studies have also had issues with the amplification of IL31 in the skin of atopic dogs.[84] Interleukin-31 can be produced and secreted by mast cells in culture.[85] We have utilized qRT-PCR to detect IL31 levels in 6-hour and 24-hour compound 48/80 samples; unfortunately, it was unsuccessful as healthy skin did not harbor any IL31 expression. We have detected IL31 expression in compound 48/80 induced skin lesions, but we could not quantify the IL3 expression since healthy skin showed no expression. Further studies using immunohistochemistry of immunofluorescence to target IL31 protein presence can be performed to elucidate the presence of IL31 in MRGPRX2 activated skin lesions.

A growing body of evidence suggests a pathogenic role for proinflammatory T helper 17 lymphocytes (Th17) in humans' chronic inflammatory skin diseases, such as psoriasis and AD.[86] The cytokines of the IL17 family include IL17A and IL17F, which are activated lymphocyte products, and IL17E and IL17C, which are epidermal keratinocytes and other types of nonimmune cell products.[86] The receptor subunits of IL17RA and IL17RE are expressed in keratinocytes and T lymphocytes where IL17C is signaled through.[86] Therefore, IL17C plays a role in both autocrine and paracrine signaling in the epidermis and to immune cells, respectively.[86] The keratinocytes produce a unique cytokine, IL17C, which is upregulated in the spontaneous AD of humans; and involved in synergistic loops that may be responsible for AD

inflammation amplification.[86] Interestingly, MRGPRX2 activation by compound 48/80 led to a significant upregulation of IL17C but not IL17A or IL17F.

One hallmark of spontaneous AD is the disturbed skin barrier function, leading to increases in skin permeability and allergen penetration.[87] Skin barrier defects in AD are observed when disturbances develop in epidermal maturation and keratinocyte differentiation, alteration of skin lipid composition and organization, and downregulation of tight junctions (TJs) in the stratum granulosum.[88] Although mutation in keratinocyte structural proteins has been observed with an increased prevalence of AD in some human patients, it is still ambiguous if barrier defects are a primary effect of AD or secondary to inflammatory processes in the epidermis and dermis.[89] There have been no investigations evaluating the effect of cutaneous inflammatory pathways on skin barrier function in dogs. Our results show that saline and compound 48/80 induce changes in the expression of epidermal skin barrier proteins, lipids, and tight junction proteins of healthy dogs. Both compound 48/80 and saline intradermal injection at 6 hours downregulated structural proteins of cornfield envelope loricrin and filaggrin 2 as well as proteins of TJs claudin 1, 8, and 10.; the effect of compound 48/80 on the skin barrier was more pronounced. A compensatory upregulation feedback mechanism of skin barrier proteins was observed in compound 48/80 skin lesions at 24 hours; there was a significant increase in expression of structural keratinocyte proteins keratin 1 and 10 as well as protease caspase 14 and transglutaminases 1 and 3. Epidermal caspase 14 converts free amino acids, including arginine, histidine, and glutamine, into pyrrolidine carboxylic acid (PCA) and urocanic acid (UCA)[90], which are the body's natural moisturizing factors (NMFs)[91], and are crucial for the barrier function of the stratum corneum. In summary, our results show that support the hypothesis that

skin barrier dysfunction can be associated with cutaneous inflammatory processes, which is in line with the data from spontaneous human AD.

We observed activation of several itch-inducing substances in compound 48/80-induced skin lesions such as mast cell secretory granules, histamine, cathepsins, MRGPRs, NGF, and leukotriene proteins. The activation of MRGPRX2 in canine skin induced upregulation of mast cell proteases chymase (CMA1), tryptase (LOC100049001), and mastin (LOC448801). Previously, an acute canine AD skin gene, mastin, exhibited to be upregulated[73] similarly to ours; however, the pathogenesis of mastin activation has not been in-depth investigated in spontaneous human and canine AD at the time.

Both serine and cysteine proteases have been implicated in triggering itch and inflammation in the skin.[92] A significant upregulation of cathepsins S (CTSS) and cathepsins C (CTSC) was observed in MRGPRX2-activated skin lesions. A lysosomal cysteine protease, CTSS, in alveolar macrophages function as an elastase over a wide-ranging pH and may play a role in antigenic protein degradation to peptides for major histocompatibility complex (MHC) class II molecule presentation.[93] Recently, CTSS was shown to activate human protease-activated receptor-2 (PAR2) and MRGPRX2, which may play a pruritic role in inflammatory skin diseases such as AD.[94]

Nerve growth factor (NGF) was another strongly upregulated pruritogen in compound 48/80-indued skin lesions at 6 and 24 hours. The keratinocyte's major mitogen, NGF, is considered more potent than the epidermal growth factor (EGF).[95] NGF is produced by keratinocytes, lymphocytes, mast cells, and other cellular components; and is critical to the growth and maintenance of neurons.[95] The nerve growth factor is considered an AD activity index and has levels that reflect the severity of the AD disease in the stratum corneum.[95]

CHAPTER 6

CONCLUSION

Overall, our data showed that MRGPRX2-activated skin lesions are characterized by an increase of Th1 and Th2 axes with decrease Th17 markers. We observed various upregulated pruritogens, including proteases, histamine, leukotrienes, and neurotrophins in canine skin lesions. We also identified that cutaneous inflammatory processes induced by MRGPRX2 activation in canine skin downregulate skin barrier genes and lead to barrier dysfunction. Limitations of this study included small sample size, induction of acute lesions vs. chronic spontaneous AD lesions, limited genomic data on converting all human genes to canine orthologues, and induction of AD lesions vs. naturally occurring AD lesions. Future studies should focus on modeling MRGPRX2 activation in atopic skin in larger populations. Furthermore, this study's results provide a rationale for investigating MRGPRX2 inhibitor as a future AD targeted therapeutics.

REFERENCES

1. Ali H. Mas-related G protein coupled receptor-X2: A potential new target for modulating mast cell-mediated allergic and inflammatory diseases. *J Immunobiol* 2016;1.

2. Subramanian H, Gupta K, Ali H. Roles of Mas-related G protein-coupled receptor X2 on mast cell-mediated host defense, pseudoallergic drug reactions, and chronic inflammatory diseases. *J Allergy Clin Immunol* 2016;138:700-710.

3. Meixiong J, Anderson M, Limjunyawong N, et al. Activation of Mast-Cell-Expressed Mas-Related G-Protein-Coupled Receptors Drives Non-histaminergic Itch. *Immunity* 2019;50:1163-1171 e1165.

4. Moon TC, Befus AD, Kulka M. Mast cell mediators: their differential release and the secretory pathways involved. *Front Immunol* 2014;5:569.

5. Voisin T, Chiu IM. Mast Cells Get on Your Nerves in Itch. *Immunity* 2019;50:1117-1119.

6. Ali H. Emerging Roles for MAS-Related G Protein-Coupled Receptor-X2 in Host Defense Peptide, Opioid, and Neuropeptide-Mediated Inflammatory Reactions. *Adv Immunol* 2017;136:123-162.

7. Gaudenzio N, Sibilano R, Marichal T, et al. Different activation signals induce distinct mast cell degranulation strategies. *J Clin Invest* 2016;126:3981-3998.

8. Hill PB, Hillier A, Olivry T. The ACVD task force on canine atopic dermatitis (VI): IgE-induced immediate and late-phase reactions, two inflammatory sequences at sites of intradermal allergen injections. *Vet Immunol Immunopathol* 2001;81:199-204.

9. Wang F, Yang T-LB, Kim BS. The Return of the Mast Cell: New Roles in Neuroimmune Itch Biology. *Journal of Investigative Dermatology* 2020.

10. Pucheu-Haston CM, Shuster D, Olivry T, et al. A canine model of cutaneous late-phase reactions: prednisolone inhibition of cellular and cytokine responses. *Immunology* 2006;117:177-187.

11. Blubaugh A, Denley T, Banovic F. Characterization of a chloroquine-induced canine model of pruritus and skin inflammation. *Vet Dermatol* 2019.

12. Blubaugh A, Rissi D, Elder D, et al. The anti-inflammatory effect of topical tofacitinib on immediate and late-phase cutaneous allergic reactions in dogs: a placebo-controlled pilot study. *Vet Dermatol* 2018;29:250-e293.

13. Blubaugh A, Denley T, Rissi D, et al. Characterization of the pro-inflammatory and pruritogenic transcriptome in experimental acute canine IgE-mediated skin lesions. *Veterinary Dermatology* 2019;30:453-469.

14. Dong X, Han S, Zylka MJ, et al. A diverse family of GPCRs expressed in specific subsets of nociceptive sensory neurons. *Cell* 2001;106:619-632.

15. Meixiong J, Dong X. Mas-Related G Protein-Coupled Receptors and the Biology of Itch Sensation. *Annu Rev Genet* 2017;51:103-121.

16. Premzl M. Comparative genomic analysis of eutherian Mas-related G protein-coupled receptor genes. *Gene* 2014;540:16-19.

17. Hamamura-Yasuno E, Iguchi T, Kumagai K, et al. Identification of the dog orthologue of human MAS-related G protein coupled receptor X2 (MRGPRX2) essential for drug-induced pseudo-allergic reactions. *Scientific Reports* 2020;10:16146.

18. Bader M, Alenina N, Andrade-Navarro MA, et al. MAS and its related G protein-coupled receptors, Mrgprs. *Pharmacol Rev* 2014;66:1080-1105.

19. Van Hagen PM, Dalm VA, Staal F, et al. The role of cortistatin in the human immune system. *Mol Cell Endocrinol* 2008;286:141-147.

20. Wedi B, Gehring M, Kapp A. The pseudoallergen receptor MRGPRX2 on peripheral blood basophils and eosinophils: expression and function. *Allergy* 2020.

21. Azimi E, Reddy VB, Lerner EA. Brief communication: MRGPRX2, atopic dermatitis and red man syndrome. *Itch (Philadelphia, Pa)* 2017;2:e5-e5.

22. Perner C, Flayer CH, Zhu X, et al. Substance P Release by Sensory Neurons Triggers Dendritic Cell Migration and Initiates the Type-2 Immune Response to Allergens. *Immunity* 2020.

23. Kühn H, Kolkhir P, Babina M, et al. Mas-related G protein-coupled receptor X2 and its activators in dermatologic allergies. *J Allergy Clin Immunol* 2020.

24. Tatemoto K, Nozaki Y, Tsuda R, et al. Endogenous protein and enzyme fragments induce immunoglobulin E-independent activation of mast cells via a G protein-coupled receptor, MRGPRX2. *Scand J Immunol* 2018;87:e12655.

25. Tatemoto K, Nozaki Y, Tsuda R, et al. Immunoglobulin E-independent activation of mast cell is mediated by Mrg receptors. *Biochem Biophys Res Commun* 2006;349:1322-1328.

26. McNeil BD, Pundir P, Meeker S, et al. Identification of a mast-cell-specific receptor crucial for pseudo-allergic drug reactions. *Nature* 2015;519:237-241.

27. Ogasawara H, Furuno M, Edamura K, et al. Peptides of major basic protein and eosinophil cationic protein activate human mast cells. *Biochem Biophys Rep* 2020;21:100719.

28. Grimes J, Desai S, Charter NW, et al. MrgX2 is a promiscuous receptor for basic peptides causing mast cell pseudo-allergic and anaphylactoid reactions. *Pharmacol Res Perspect* 2019;7:e00547.

29. Wang J, Zhang Y, Che D, et al. Baicalin induces Mrgprb2-dependent pseudo-allergy in mice. *Immunology Letters* 2020;226:55-61.

30. McNeil B, Dong X. Mrgprs as Itch Receptors In: Carstens E,Akiyama T, eds. *Itch: Mechanisms and Treatment*. Boca Raton (FL), 2014.

31. Wang Z, Babina M. MRGPRX2 signals its importance in cutaneous mast cell biology: Does MRGPRX2 connect mast cells and atopic dermatitis? *Experimental Dermatology* 2020;n/a.

32. Bulfone-Paus S, Nilsson G, Draber P, et al. Positive and Negative Signals in Mast Cell Activation. *Trends Immunol* 2017;38:657-667.

33. Kiatsurayanon C, Niyonsaba F, Chieosilapatham P, et al. Angiogenic peptide (AG)-30/5C activates human keratinocytes to produce cytokines/chemokines and to migrate and proliferate via MrgX receptors. *J Dermatol Sci* 2016;83:190-199.

34. Varricchi G, Pecoraro A, Loffredo S, et al. Heterogeneity of Human Mast Cells With Respect to MRGPRX2 Receptor Expression and Function. *Front Cell Neurosci* 2019;13:299.

35. Porebski G, Kwiecien K, Pawica M, et al. Mas-Related G Protein-Coupled Receptor-X2 (MRGPRX2) in Drug Hypersensitivity Reactions. *Front Immunol* 2018;9:3027.

36. Motakis E, Guhl S, Ishizu Y, et al. Redefinition of the human mast cell transcriptome by deep-CAGE sequencing. *Blood* 2014;123:e58-e67.

37. Lansu K, Karpiak J, Liu J, et al. In silico design of novel probes for the atypical opioid receptor MRGPRX2. *Nat Chem Biol* 2017;13:529-536.

38. Yosipovitch G, Rosen JD, Hashimoto T. Itch: From mechanism to (novel) therapeutic approaches. *J Allergy Clin Immunol* 2018;142:1375-1390.

39. Kirshenbaum AS, Yin Y, Sundstrom JB, et al. Description and Characterization of a Novel Human Mast Cell Line for Scientific Study. *International journal of molecular sciences* 2019;20:5520.

40. Kulka M, Sheen CH, Tancowny BP, et al. Neuropeptides activate human mast cell degranulation and chemokine production. *Immunology* 2008;123:398-410.

41. Serhan N, Basso L, Sibilano R, et al. House dust mites activate nociceptor-mast cell clusters to drive type 2 skin inflammation. *Nat Immunol* 2019;20:1435-1443.

42. Fujisawa D, Kashiwakura J, Kita H, et al. Expression of Mas-related gene X2 on mast cells is upregulated in the skin of patients with severe chronic urticaria. *J Allergy Clin Immunol* 2014;134:622-633.e629.

43. Arroyo-Mercado F, Khudyakov A, Chawla GS, et al. Red Man Syndrome with Oral Vancomycin: A Case Report. *Am J Med Case Rep* 2019;7:16-17.

44. Bergeron L, Boucher FD. Possible red-man syndrome associated with systemic absorption of oral vancomycin in a child with normal renal function. *Ann Pharmacother* 1994;28:581-584.

45. Domis MJ, Moritz ML. Red man syndrome following intraperitoneal vancomycin in a child with peritonitis. *Front Pediatr* 2014;2:55.

46. Sivagnanam S, Deleu D. Red man syndrome. *Crit Care* 2003;7:119-120.

47. Bernstein JA, Lang DM, Khan DA, et al. The diagnosis and management of acute and chronic urticaria: 2014 update. *J Allergy Clin Immunol* 2014;133:1270-1277.

48. Marsella R, De Benedetto A. Atopic Dermatitis in Animals and People: An Update and Comparative Review. *Vet Sci* 2017;4.

49. Yang G, Seok JK, Kang HC, et al. Skin Barrier Abnormalities and Immune Dysfunction in Atopic Dermatitis. *International journal of molecular sciences* 2020;21:2867.

50. Brunner PM, Guttman-Yassky E, Leung DYM. The immunology of atopic dermatitis and its reversibility with broad-spectrum and targeted therapies. *The Journal of allergy and clinical immunology* 2017;139:S65-S76.

51. Tokura Y. Extrinsic and intrinsic types of atopic dermatitis. *J Dermatol Sci* 2010;58:1-7.

52. Steinhoff M, Buddenkotte J, Lerner EA. Role of mast cells and basophils in pruritus. *Immunol Rev* 2018;282:248-264.

53. Bieber T. Interleukin-13: Targeting an underestimated cytokine in atopic dermatitis. *Allergy* 2020;75:54-62.

54. Nakamura Y, Oscherwitz J, Cease KB, et al. Staphylococcus delta-toxin induces allergic skin disease by activating mast cells. *Nature* 2013;503:397-401.

55. Bell A, Nakamura Y, Langley R, et al. Canine mast cell degranulation induced by a newly identified toxin from Staphylococcus pseudintermedius. *Veterinary Dermatology* 2017;28:426-455.

56. Bumbacea RS, Corcea SL, Ali S, et al. Mite allergy and atopic dermatitis: Is there a clear link? (Review). *Experimental and therapeutic medicine* 2020;20:3554-3560.

57. Mason IS, Lloyd DH. Evaluation of compound 48/80 as a model of immediate hypersensitivity in the skin of dogs. *Veterinary Dermatology* 1996;7:81-83.

58. Vogelnest LJ, Mueller RS, Dart CM. The suitability of medetomidine sedation for intradermal skin testing in dogs. *Veterinary Dermatology* 2000;11:285-290.

59. Hillier A, DeBoer DJ. The ACVD task force on canine atopic dermatitis (XVII): intradermal testing. *Vet Immunol Immunopathol* 2001;81:289-304.

60. Baumer W, Rossbach K, Schmidt BH. The selective glucocorticoid receptor agonist mapracorat displays a favourable safety-efficacy ratio for the topical treatment of inflammatory skin diseases in dogs. *Vet Dermatol* 2017;28:46-e11.

61. Bizikova P, Linder KE, Paps J, et al. Effect of a novel topical diester glucocorticoid spray on immediate- and late-phase cutaneous allergic reactions in Maltese-beagle atopic dogs: a placebo-controlled study. *Vet Dermatol* 2010;21:70-79.

62. Banovic F, Denley T, Blubaugh A. Dose-dependent pruritogenic and inflammatory effects of intradermal injections of histamine, compound 48/80 and anti-canine IgE in healthy dogs. *Vet Dermatol* 2019;30:325-e391.

63. Banovic F, Denley T, Blubaugh A, et al. Effect of diphenhydramine and cetirizine on immediate and late-phase cutaneous allergic reactions in healthy dogs: a randomized, double-blinded crossover study. *Vet Dermatol* 2020.

64. S. A. FastQC: A Quality Control Tool for High Throughput Sequence Data 2010.

65. Bolger AM, Lohse M, Usadel B. Trimmomatic: a flexible trimmer for Illumina sequence data. *Bioinformatics* 2014;30:2114-2120.

66. Kim D, Pertea G, Trapnell C, et al. TopHat2: accurate alignment of transcriptomes in the presence of insertions, deletions and gene fusions. *Genome Biol* 2013;14:R36.

67. Langmead B, Salzberg SL. Fast gapped-read alignment with Bowtie 2. *Nat Methods* 2012;9:357-359.

68. Anders S, Huber W. Differential expression analysis for sequence count data. *Genome Biol* 2010;11:R106.

69. Benjamini Y, Hochberg Y. Controlling the False Discovery Rate: A Practical and Powerful Approach to Multiple Testing. *Journal of the Royal Statistical Society Series B (Methodological)* 1995;57:289-300.

70. Freudenberg JM, Joshi VK, Hu Z, et al. CLEAN: CLustering Enrichment ANalysis. *BMC Bioinformatics* 2009;10:234.

71. Hänzelmann S, Castelo R, Guinney J. GSVA: gene set variation analysis for microarray and RNA-Seq data. *BMC Bioinformatics* 2013;14:7.

72. Tsoi LC, Rodriguez E, Degenhardt F, et al. Atopic Dermatitis Is an IL-13-Dominant Disease with Greater Molecular Heterogeneity Compared to Psoriasis. *J Invest Dermatol* 2019;139:1480-1489.

73. Plager DA, Torres SM, Koch SN, et al. Gene transcription abnormalities in canine atopic dermatitis and related human eosinophilic allergic diseases. *Vet Immunol Immunopathol* 2012;149:136-142.

74. Huber W, Carey VJ, Gentleman R, et al. Orchestrating high-throughput genomic analysis with Bioconductor. *Nat Methods* 2015;12:115-121.

75. Parman CH CG, R. . affyQCReport: QC Report Generation for affyBatch objects. 1.48.0 ed2017. p. R package (version 1.48.0). 2017.

76. Brunner PM, Israel A, Zhang N, et al. Early-onset pediatric atopic dermatitis is characterized by T(H)2/T(H)17/T(H)22-centered inflammation and lipid alterations. *J Allergy Clin Immunol* 2018;141:2094-2106.

77. Guttman-Yassky E, Ungar B, Noda S, et al. Extensive alopecia areata is reversed by IL-12/IL-23p40 cytokine antagonism. *Journal of Allergy and Clinical Immunology* 2016;137:301-304.

78. Dhingra N, Shemer A, Correa da Rosa J, et al. Molecular profiling of contact dermatitis skin identifies allergen-dependent differences in immune response. *Journal of Allergy and Clinical Immunology* 2014;134:362-372.

79. Ewald DA, Noda S, Oliva M, et al. Major differences between human atopic dermatitis and murine models, as determined by using global transcriptomic profiling. *J Allergy Clin Immunol* 2017;139:562-571.

80. Noda S, Suárez-Fariñas M, Ungar B, et al. The Asian atopic dermatitis phenotype combines features of atopic dermatitis and psoriasis with increased TH17 polarization. *J Allergy Clin Immunol* 2015;136:1254-1264.

81. Gittler JK, Shemer A, Suarez-Farinas M, et al. Progressive activation of T(H)2/T(H)22 cytokines and selective epidermal proteins characterizes acute and chronic atopic dermatitis. *J Allergy Clin Immunol* 2012;130:1344-1354.

82. Tsoi LC, Rodriguez E, Stolzl D, et al. Progression of acute-to-chronic atopic dermatitis is associated with quantitative rather than qualitative changes in cytokine responses. *J Allergy Clin Immunol* 2019.

83. Altrichter S, Frischbutter S, Fok JS, et al. The role of eosinophils in chronic spontaneous urticaria. *J Allergy Clin Immunol* 2020;145:1510-1516.

84. McCandless EE, Rugg CA, Fici GJ, et al. Allergen-induced production of IL-31 by canine Th2 cells and identification of immune, skin, and neuronal target cells. *Veterinary Immunology and Immunopathology* 2014;157:42-48.

85. Petra AI, Tsilioni I, Taracanova A, et al. Interleukin 33 and interleukin 4 regulate interleukin 31 gene expression and secretion from human laboratory of allergic diseases 2 mast cells stimulated by substance P and/or immunoglobulin E. *Allergy and asthma proceedings* 2018;39:153-160.

86. Guttman-Yassky E, Krueger JG. IL-17C: A Unique Epithelial Cytokine with Potential for Targeting across the Spectrum of Atopic Dermatitis and Psoriasis. *Journal of Investigative Dermatology* 2018;138:1467-1469.

87. Gittler JK, Krueger JG, Guttman-Yassky E. Atopic dermatitis results in intrinsic barrier and immune abnormalities: implications for contact dermatitis. *The Journal of allergy and clinical immunology* 2013;131:300-313.

88. Hönzke S, Wallmeyer L, Ostrowski A, et al. Influence of Th2 Cytokines on the Cornified Envelope, Tight Junction Proteins, and β-Defensins in Filaggrin-Deficient Skin Equivalents. *Journal of Investigative Dermatology* 2016;136:631-639.

89. Marsella R, Olivry T, Carlotti D-N, et al. Current evidence of skin barrier dysfunction in human and canine atopic dermatitis. *Veterinary Dermatology* 2011;22:239-248.

90. Egawa G, Kabashima K. Multifactorial skin barrier deficiency and atopic dermatitis: Essential topics to prevent the atopic march. *J Allergy Clin Immunol* 2016;138:350-358.e351.

91. Hoste E, Kemperman P, Devos M, et al. Caspase-14 is required for filaggrin degradation to natural moisturizing factors in the skin. *J Invest Dermatol* 2011;131:2233-2241.

92. Reddy VB, Sun S, Azimi E, et al. Redefining the concept of protease-activated receptors: cathepsin S evokes itch via activation of Mrgprs. *Nature Communications* 2015;6:7864.

93. Kim N, Bae KB, Kim MO, et al. Overexpression of Cathepsin S Induces Chronic Atopic Dermatitis in Mice. *Journal of Investigative Dermatology* 2012;132:1169-1176.

94. Reddy VB, Shimada SG, Sikand P, et al. Cathepsin S Elicits Itch and Signals via Protease-Activated Receptors. *Journal of Investigative Dermatology* 2010;130:1468-1470.

95. Gaspar NK, Aidé MK. Atopic dermatitis: allergic dermatitis or neuroimmune dermatitis? *Anais brasileiros de dermatologia* 2016;91:479-488.